

Blockade of YAP Mechanoactivation Prevents Neointima Formation and Adverse Remodeling in Arterialized Vein Grafts

*Original*

Blockade of YAP Mechanoactivation Prevents Neointima Formation and Adverse Remodeling in Arterialized Vein Grafts / Garoffolo, G., Sluiter, T.J., Thomas, A., Piacentini, L., Ruitter, M.S., Schiavo, A., Salvi, M., Saccu, C., Zoli, S., Chiesa, M., Yokoyama, T., Agrifoglio, M., Soncini, M., Fiore, G.B., Martelli, F., Condorelli, G., Madeddu, P., Molinari, F., Morbiducci, U., Quax, P.H.A., et al.. - In: JOURNAL OF THE AMERICAN HEART ASSOCIATION. CARDIOVASCULAR AND CEREBROVASCULAR DISEASE. - ISSN 2047-9980. - (2025). [10.1161/jaha.124.037531]

*Availability:*

This version is available at: 11583/2998501 since: 2025-03-22T13:03:58Z

*Publisher:*

Wiley

*Published*

DOI:10.1161/jaha.124.037531

*Terms of use:*

This article is made available under terms and conditions as specified in the corresponding bibliographic description in the repository

*Publisher copyright*

(Article begins on next page)

ORIGINAL RESEARCH

# Blockade of YAP Mechanoactivation Prevents Neointima Formation and Adverse Remodeling in Arterialized Vein Grafts

Gloria Garoffolo, PhD; Thijs J. Sluiter , PhD; Anita Thomas , PhD; Luca Piacentini , PhD; Matthijs S. Ruiters , PhD; Alessia Schiavo, MSc; Massimo Salvi , PhD; Claudio Saccu , MD; Stefano Zoli, MD; Mattia Chiesa , PhD; Takumi Yokoyama, PhD; Marco Agrifoglio , MD, PhD; Monica Soncini , PhD; Gianfranco B. Fiore , PhD; Fabio Martelli , PhD; Gianluigi Condorelli , MD, PhD; Paolo Madeddu , MD, PhD; Filippo Molinari , PhD; Umberto Morbiducci , PhD; Paul H. A. Quax , PhD; Gaia Spinetti , PhD; Margreet R. de Vries , PhD; Maurizio Pesce , PhD

**BACKGROUND:** Bypass surgery using saphenous vein (SV) grafts is commonly performed to revascularize the ischemic heart and lower limbs. These interventions have limited success due to adverse remodeling caused by overproliferation of smooth muscle cells in the intima layer, leading to progressive bypass stenosis. We previously showed that cyclic strain deriving from exposure to coronary flow induces the expression of the matricellular protein thrombospondin-1 in the human SV, promoting activation of progenitor cells normally residing in the adventitia.

**METHODS:** We analyzed the data of an RNA-sequencing profiling of human SV progenitors subjected to uniaxial strain we previously performed by. Experiments in cell culture, ex vivo, and in vivo vein arterialization models were performed to substantiate findings with particular reference to the role of mechanically activated transcription factors. Validation was performed in vitro and in ex vivo/in vivo models of vein graft disease.

**RESULTS:** Results of bioinformatic assessment of the RNA-sequencing data indicated Yes-associated protein (YAP) as a possible mechanically regulated effector in pathologic evolution of SV progenitors. Inhibition of YAP by verteporfin—a drug that abolishes the interaction of YAP with Tea Domain DNA-binding proteins—reduced the expression of pathologic markers in vitro and reduced intima hyperplasia in vivo.

**CONCLUSIONS:** Our results reveal that desensitizing the SV-resident cells to mechanoactivation of YAP is feasible to reduce the graft disease progression.

**Key Words:** mechanical strain ■ TGF- $\beta$  ■ vein graft disease ■ verteporfin ■ YAP

Despite the high performance of percutaneous coronary interventions and the superiority of arterial conduits (eg, the inner mammary artery or the radial artery) in maintaining graft patency at mid/long term,<sup>1</sup> the use of venous bypass conduits remains common in coronary surgery,<sup>2</sup> especially in multivessel coronary artery disease.<sup>3</sup> Vein grafts are

also frequently used in the surgical treatment of peripheral artery disease, where saphenous vein (SV) implantation is superior to endovascular treatment.<sup>4</sup> While the choice of SV is justified by ease of harvesting, length, manufacturability, and excellent mechanical resistance, it also has limitations deriving from a maladaptive remodeling process that initiates

Correspondence to: Maurizio Pesce, PhD, Centro Cardiologico Monzino, IRCCS, Unità di Ingegneria Tissutale, Via C. Parea, 4, Milan 20138, Italy. Email: [maurizio.pesce@cardiologicomonzino.it](mailto:maurizio.pesce@cardiologicomonzino.it) and [mpesce@kfshrc.edu.sa](mailto:mpesce@kfshrc.edu.sa)

This article was sent to June-Wha Rhee, MD, Associate Editor, for review by expert referees, editorial decision, and final disposition.

Supplemental Material is available at <https://www.ahajournals.org/doi/suppl/10.1161/JAHA.124.037531>

For Sources of Funding and Disclosures, see page 13.

© 2025 The Author(s). Published on behalf of the American Heart Association, Inc., by Wiley. This is an open access article under the terms of the [Creative Commons Attribution-NonCommercial-NoDerivs](https://creativecommons.org/licenses/by-nc-nd/4.0/) License, which permits use and distribution in any medium, provided the original work is properly cited, the use is non-commercial and no modifications or adaptations are made.

JAHA is available at: [www.ahajournals.org/journal/jaha](http://www.ahajournals.org/journal/jaha)

## CLINICAL PERSPECTIVE

### What Is New?

- With this contribution, we demonstrate the involvement of the mechanically activated Yes-associated protein pathway in the pathological remodeling of the venous coronary artery bypasses.

### What Are the Clinical Implications?

- We show the feasibility of a “mechanotherapeutic” approach to reduce the impact of vein graft disease by pharmacologically targeting molecular pathways involved in cellular mechanosensation.

## Nonstandard Abbreviations and Acronyms

<b>CCL2</b>	C-C motif ligand 2
<b>FN</b>	fibronectin
<b>FRSK</b>	forskolin
<b>MCP-1</b>	monocyte chemoattractant protein-1
<b>p53</b>	tumor protein p53
<b>RT-qPCR</b>	real-time quantitative polymerase chain reaction
<b>SV</b>	saphenous vein
<b>SVP</b>	saphenous vein progenitor
<b>TAZ</b>	PDZ-binding motif
<b>TEAD</b>	TEA domain transcription factor
<b>TGF-<math>\beta</math></b>	transforming growth factor $\beta$
<b>TIMP-3</b>	tissue inhibitor of metalloproteinases-3
<b>TSP-1</b>	thrombospondin 1
<b>VGD</b>	vein graft disease
<b>VTP</b>	verteporfin
<b>YAP</b>	Yes-associated protein

shortly after implantation. This triggers progressive occlusion and formation of atherosclerotic plaques in a high percentage of patients. This process, known as vein graft disease (VGD), has various pathophysiological causes, including mechanical damage to the endothelium or the vessel wall due to physical manipulation during harvest, exposure to the high arterial pressure/flow regimen, hypoxia, intraplaque angiogenesis, inflammation, lipid accumulation, and secondary atherosclerosis.<sup>5–7</sup>

At a cell biology level, VGD is caused by overproliferation of cells with smooth muscle cell (SMC)-like characteristics in the vein wall. These cells may originate from preexisting SMCs that undergo a phenotypic

switch from contractile to secretory or from progenitors residing in the adventitia,<sup>8–10</sup> which migrate towards the subendothelial (intima) layer and accumulate to reduce the patency of the graft by an “inward” growing process.<sup>5</sup> Extensive research has highlighted several molecular effectors potentially involved in SV maladaptive remodeling. These include innate immunity effectors, chemokines, and matrix-remodeling enzymes.<sup>7</sup> Unfortunately, the success of targeting these factors to reduce VGD in patients has been limited.<sup>6,11,12</sup> In an effort to delineate novel pathophysiological mechanisms in VGD, we implemented a bioengineering approach to assess the role of mechanical forces in the failure of SV coronary artery bypass grafts. We previously found that exposure of human SVs to pulsatile coronary-like flow<sup>13</sup> generates matricellular signaling mediated by transforming growth factor  $\beta$ 1 (TGF- $\beta$ 1) and thrombospondin-1 (TSP-1), which recruits resident progenitors with SMC-like characteristics to initiate the process of vascular remodeling.<sup>14</sup>

In the present study, we employed RNA sequencing to identify mechanically activated transcriptional pathways connected to direct myofibroblast differentiation of these progenitors.<sup>15,16</sup> We identified numerous genes that are modulated by mechanical stimulation, including those involved in the transcriptional network dependent on YAP, a key transcription factor within the Hippo pathway.<sup>17,18</sup> Cell biology experiments confirmed the involvement of YAP in the acquisition of a myofibroblast phenotype.<sup>19</sup> To reduce mechanical activation of adventitial progenitors, we utilized verteporfin (VTP), an inhibitor of the transcriptional complex formed by YAP and the transcriptional coactivator with PDZ-binding motif (TAZ) complex, which we recently found to inhibit fibrosis in the ischemic heart<sup>20</sup> and reduce pathologic activation of human valve interstitial cells.<sup>21</sup> SV progenitors (SVPs) treated with the drug exhibited reduced migratory ability and formation of focal adhesion contacts.<sup>22</sup> VTP also reduced the interaction of YAP with phospho-SMAD3 (pSMAD3), a transcriptional activator downstream of TGF- $\beta$ 1, while blunting the expression of  $\alpha$ SMA, TSP-1, and fibronectin (FN) and significantly inhibiting the expression/secretion of collagen. Finally, VTP substantially reduced the extent of fibrosis and adverse remodeling in a mouse model of vein graft failure.<sup>23</sup>

## METHODS

A complete methodological section is available in Data S1. Lists of the primers sequences and antibodies used in the study are provided in Tables S1 and S2, respectively. The data that support the findings of this study are available from the corresponding author upon reasonable request.

## Ethical Statement of In Vivo Procedures

The use of human SV material (recovered during sa-phenectomy or harvesting for coronary artery bypass grafts, patient characteristics in [Table S3](#)) for ex vivo experiments and cell culture was authorized by the ethical committee at Centro Cardiologico Monzino, IRCCS. Patients were required to sign an informed consent. The use of human material was performed in compliance with the Declaration of Helsinki. For the in vivo SV arterIALIZATION model in pigs,<sup>24</sup> animals received humane care in accordance with the Home Office Animals (Scientific Procedures) Act of 1986 and the Guide for the Care and Use of Laboratory Animals published by the US National Institutes of Health (NIH publication number 85–23, revised 1996). The trial of vena cava to carotid artery transplantation in mice was performed according to an experimental procedure authorized by the institutional committee of the Leiden University Medical Center, which approved all animal experiments licensed under project number (AVD1160020172409). These animal experiments were performed in compliance with Dutch government guidelines and the Directive 2010/63/EU of the European Parliament.

## Statistical Analysis

The statistical analyses supporting the bioinformatics analysis of the RNA sequencing data are reported in the specific section of the extended online methods. The type of statistical tests to compare data presented in the bar graphs throughout the study are specified in the figure legends. Each bar includes the number of experimental replicates (performed on independent mice and cell lines), and a  $P$  value  $<0.05$  was considered significant for statistical comparisons. Data were analyzed using GraphPad software. All data are represented as mean  $\pm$  standard error of the mean. Before performing statistical analyses, normality and outliers' tests were performed. The type of statistical test used to compare data is specified in the legend of each figure. For single comparisons, we used 2-tailed paired or unpaired  $t$  tests. For multiple comparisons, we used 1-way ANOVA with Tukey or Dunnett post hoc. Differential gene expression in RNA sequencing analysis were corrected by the Benjamini-Hochberg method, considering differentially expressed genes, with an adjusted  $P$  value  $<0.05$ . Further details are displayed in the figure legends and supplementary material.

## RESULTS

### Cyclic Strain-Dependent Gene Regulation in Human SVPs Increases YAP Transcriptional Signaling

We assessed the general effects of uniaxial strain-ing on the global transcriptome of human adventitial

progenitors.<sup>15,16</sup> The condition of mechanically stimulated versus statically cultured SVPs (“ON” versus “OFF” comparisons) determined reorientation of the cells along a preferentially orthogonal direction to the strain field and changes in cellular form factors ([Figure 1A](#)). RNA sequencing performed using total RNA from mechanically stimulated (ON) versus statically cultured (OFF) cells for 72 hours highlighted several hundred modulated genes ([Figure 1B](#)).<sup>25</sup> In order to derive a signature of the mechanically regulated genes, we performed a differential gene expression analysis. This resulted in a list of 155 upregulated and 259 downregulated genes ( $|\log_2FC|>1$  and adjusted  $P$  value  $<0.05$ ; Dataset [S1](#)) in the mechanically stimulated versus static cultured cells (ON versus OFF condition). Gene Ontology enrichment analysis showed the presence of mechanically regulated pathways ([Figure 1C](#)), including genes related to extracellular matrix organization, cell adhesion to matrix components, proliferation, and response to fibrotic signaling (Dataset [S2](#) and [S3](#)). In other cell types (eg, cardiac fibroblasts), uniaxial strain dose-dependently increases nuclear translocation of the transcription factor YAP.<sup>26</sup> We therefore directed our bioinformatic survey to assess changes in regulation of the Hippo signaling components and putative YAP transcriptional targets ([Figure 1D](#) and [Figure S1A](#)). This revealed a consistent modulation of genes functionally annotated as YAP targets and components of the Hippo pathway, according to Gene Ontology and Kyoto Encyclopedia of Genes and Genomes terms. Validation of results by real-time quantitative polymerase chain reaction (RT-qPCR) ([Figure 1D](#)) confirmed the effect of mechanical strain on the expression of key members of the TGF- $\beta$  pathway, suggesting, as previously reported,<sup>27</sup> a functional convergence involving YAP as a common determinant. However, RT-qPCR did not confirm (with the exception of *FZD8*) the relevance of genes belonging to the Wnt-activated signaling pathway as potential YAP targets affected by mechanical stimulation ([Figure S1B](#)).

To further confirm the importance of YAP in strain-dependent SVP activation, we assessed whether the morphological changes determined by the mechanic stimulation ([Figure 1A](#)) also induced nuclear translocation of the transcription factor. A clear increase in nuclear YAP was observed on mechanical activation of SVPs, indicative of YAP transcriptional activation ([Figure 1E](#)). Furthermore, mechanical stimulation decreased phosphorylation of YAP at Ser127,<sup>27</sup> which normally promotes cytoplasmic retention.<sup>28</sup> However, the nuclear translocation of YAP was not associated with an imbalance in the expression and phosphorylation levels of large tumor suppressor kinase, a component of the Hippo pathway upstream of YAP<sup>17,29,30</sup> ([Figure 1F](#)). Consistently, with the increased nuclear translocation, the expression of canonical YAP target

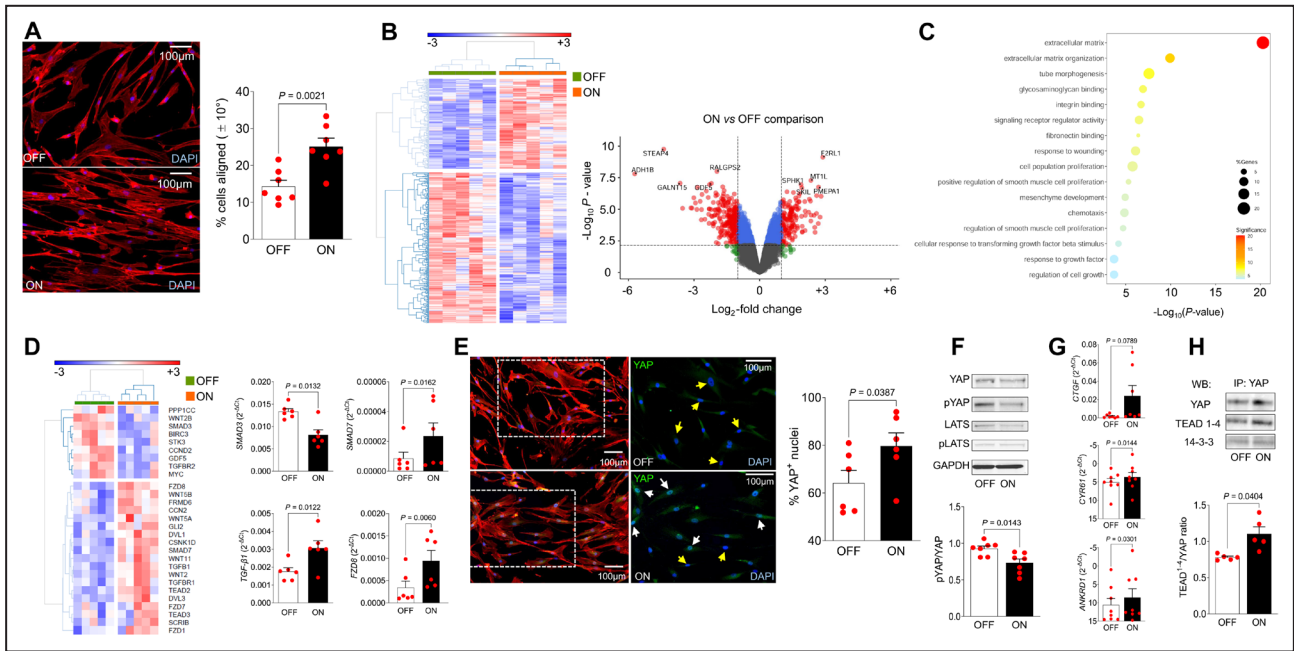


**Figure 1. Mechanosensitivity of human SVPs and activation of YAP-dependent signaling.**

**A**, Human SVPs subjected to cyclic strain (10% elongation, 1 Hz frequency) for 72 hours underwent extensive orientation changes. Cells were stained with phalloidin TRITC (red) and DAPI. The graph indicates the difference in the alignment of the major axis of the nuclei (indicative of orientation of the whole cellular body) in a perpendicular direction to the strain (vertical in the lower micrograph). **B**, Heatmap representing the results of an unsupervised cluster analysis and relative volcano plot indicating the genes that, by RNA sequencing, were found to be differentially expressed in mechanically stimulated (ON) vs statically cultured (OFF) SVPs for 72 hours. Red dots in the volcano plot represent genes that are upmodulated/downmodulated by  $|\log_2FC| > 1$ , with an adjusted  $P$  value  $< 0.05$ . **C**, Bubble plot representing upregulated Gene Ontology pathways significantly enriched in the ON vs OFF comparison. As is evident, this comparison produced enrichment of numerous pathways connected with extracellular matrix remodeling and binding and smooth muscle cells proliferation and differentiation. **D**, Unsupervised cluster analysis of the differentially expressed genes with a Hippo pathway functional annotation. The heatmap shows the majority of genes that were upregulated in the ON vs OFF condition. This included genes belonging to the TGF- $\beta$  pathways (eg, *TGFBR1*, *TGFB1*, *SMAD7*) and Wnt-dependent signaling (eg, *FZD1/8*, *WNT5A*, *GLI2*, *DVL1/3*). Part of these genes were confirmed by real-time quantitative polymerase chain reaction on independent RNA samples (see graphs on the right of the panel with indication of the significance in pairwise comparison). **E**, Effect of cyclic straining on YAP nuclear translocation. Immunofluorescence staining of cells cultured in static or dynamic conditions for 72 hours was performed with YAP-specific antibodies, followed by quantitative analysis of nYAP<sup>+</sup> and nYAP<sup>-</sup> cells (white and yellow arrows, respectively). Pairwise comparison of the 2 conditions revealed a significant increase of nYAP<sup>+</sup> cells in dynamically cultured cells. **F**, Mechanical stimulation led to a significant decrease of pYAP at Ser127. This was independent of the Hippo kinase pathway modulation, as demonstrated by an equal level of the pLATS. **G**, Assessment of canonical YAP transcriptional targets *CTGF*, *ANKRD1*, and *CTGF* expression under static and dynamic conditions establishes the role of YAP as a transcriptional mechanosensory in SVPs. **H**, TEAD 1–4, but not the 14-3-3 interaction with YAP is increased in mechanically stimulated cells, as shown by immunoprecipitation/Western analysis followed by quantification. In all graphs, red dots overlapping the bars indicate the result of each experiment performed in independent cell lines. The data represented in the bar graph in (**A**, **D**, **F**, **G**, and **H**) were compared by pairwise  $t$  test. The  $P$  values are indicated above the significance lines. DAPI indicates 4',6-diamidino-2-phenylindole; LATS, large tumor suppressor kinase; nYAP; nuclear YAP; pLATS, phosphorylated form of large tumor suppressor kinase; pYAP, phosphorylated YAP; SVP, saphenous vein progenitor; TEAD, TEA domain transcription factor; TGF- $\beta$ , transforming growth factor  $\beta$ ; TRITC, tetramethylrhodamine isothiocyanate; and YAP, Yes-associated protein.

genes *CTGF*, *CYR61*, and *ANKRD1*,<sup>20,21</sup> as well as the physical interaction with TEA domain transcription factor (TEAD) 1–4 DNA binding proteins,<sup>31</sup> was significantly increased in mechanically stimulated cells (Figure 1G and 1H), as demonstrated by RT-qPCR and by the increased intensity of the TEAD1–4 band in immunoprecipitation/Western blot analyses (see also quantification of the TEAD1–4/YAP ratio, revealed by densitometric analysis).

### YAP Function in Human SVP Is Stress Fibers-Dependent

Cytoskeleton tensioning due to transmission of mechanical forces or adhesion on geometrically patterned adhesive substrates is connected to cytoskeleton-dependent activation of YAP transcriptional signaling with variation in cell responses such as migration and proliferation.<sup>17,29</sup> We previously showed that adhesion of fibroblast-like cells

onto substrates (plastic or glass) with a Young elastic modulus in the range of Mega Pascal is, per se, a mechanically sufficient stimulus to observe robust YAP nuclear signaling caused by firm adhesion and stress fibers polymerization.<sup>20</sup> Because inhibition of F-actin by protein kinase A reduced YAP/TEAD-dependent SMC proliferation in previous studies,<sup>32</sup> we tested the effects of forskolin (FRSK), a pharmacological stimulator of cyclic adenosine monophosphate production and protein kinase A activation with direct effects on actin cytoskeleton.<sup>33</sup> Treatment with FRSK resulted in partial depolymerization of the F-actin cytoskeleton of SVPs, which was associated with a reduction in the percentage of cells that exhibited a clear nuclear localization of YAP (Figure 2A, top right). To assess how the pharmacological treatment interferes with YAP localization, we quantified YAP fluorescence using ImageJ or a proprietary algorithm (CARDiosphere Evaluation) that was devised specifically for automated segmentation of fluorescence images.<sup>34</sup> This enabled us to determine the nuclear/cytoplasm YAP expression ratio. As shown in the bottom of Figure 2A, the addition of FRSK in the medium caused a significant relocation of the YAP fluorescence from the nucleus to the cytoplasm, while removal of the drug restored YAP nuclear localization. In keeping with previous results showing that YAP nuclear localization is regulated by direct phosphorylation,<sup>35</sup> Western analysis confirmed an elevation of phospho-YAP in cells treated with FRSK (Figure 2B, left). Negative transcriptional regulation of *CTGF*, and, to a greater extent, *CYR61* and *ANKRD1*—direct YAP transcriptional targets—followed the trend of YAP nuclear shuttling in cells treated with FRSK (Figure 2B, right). Finally, to assess whether mechanical stimulation was also related to an increase in cellular motility (another cellular mechanism regulated by YAP<sup>36</sup>), we performed migration tests with SVPs exposed to cyclic strain (or not) and in the presence or the absence of protein kinase A activator. This showed that mechanically stimulated SVPs had a higher migratory ability, and this migration was inhibited by depolymerization of the cytoskeleton (Figure 2C). A more direct role of YAP and TEAD in migratory activity of SVPs was finally assessed by genetically interfering with YAP expression by treating cells with specific small interfering RNAs. As shown in Figure 2D, the use of YAP- and TEAD-specific small interfering RNAs abolished the SVPs migration, thus confirming a direct role of the YAP transcriptional function in SVP motility.

### Cooperation of YAP Signaling With TGF- $\beta$ Downstream Targets Establishes a Molecular Basis for SMC-Like Differentiation of SVPs

We previously showed that profibrotic signaling in arterialized veins might depend on a mechanically

activated pathway involving the TGF- $\beta$ /TSP-1 axis.<sup>14</sup> Therefore, we interrogated the set of the upregulated genes in SVPs in the ON versus OFF conditions, searching for targets containing known binding sequences for transcription factors. With this search we identified gene modules potentially regulated by a number of DNA-binding factors (Figure 3A, Dataset S4), among which TEAD4, one of the natural molecular interactors of the YAP/TAZ complex,<sup>37,38</sup> was enriched. A Gene Ontology analysis of the genes potentially regulated by TEAD4 in the same gene set was then performed, and this led to the identification of numerous pathways related to extracellular matrix remodeling and response to TGF- $\beta$  signaling (Figure 3B, Dataset S5). To mechanistically substantiate the convergence of YAP/TAZ and TGF- $\beta$  profibrotic signaling on mechanical-dependent activation of SVPs, we plated SVPs onto the Mega Pascal substrate with or without stimulation with TGF- $\beta$ , TSP-1, or the combination of the two (T+T condition). We then assessed the YAP nucleus/cytoplasmic ratio and determined the expression of proliferating cell nuclear antigen and SM22 $\alpha$ . Results showed that the T+T combination yielded the highest level of nuclear YAP translocation (Figure 3C) and significantly increased the growth and SMC differentiation of SVPs (Figure 3D). These findings were corroborated by an increase in phosphorylation of SMAD2 and SMAD3, the most relevant nuclear transducers of TGF- $\beta$  profibrotic signaling,<sup>39</sup> in cells treated with the T+T combination (Figure S2).

### Implication of YAP Signaling in the Vein Arterialization Process

We next investigated the direct involvement of YAP in the vein arterialization process. To this aim, we assessed the expression of the transcription factor using: (1) human SVs exposed to either venous flow or coronary flow/pressure,<sup>13,14</sup> (2) a porcine in vivo vein graft model (SV interposition in carotid),<sup>24,40</sup> and (3) a time course of murine in vivo vein graft model (caval vein interposition in carotid).<sup>23</sup> The results of immunohistochemistry staining with YAP-specific antibodies exhibited a progressive increase in the number of cells with nuclear YAP<sup>+</sup> cells, especially in the porcine and mouse models (Figure 4). It is interesting to note that cells with nuclei with a more elongated shape, apparently aligned in the direction of the circumferential component of the hemodynamic force in the graft wall,<sup>14</sup> were found to contain a higher amount of nuclear YAP. This extends our previous observations showing the effects of compression forces on nuclear YAP translocation in cardiac fibroblasts in postischemic myocardial remodeling.<sup>20</sup>

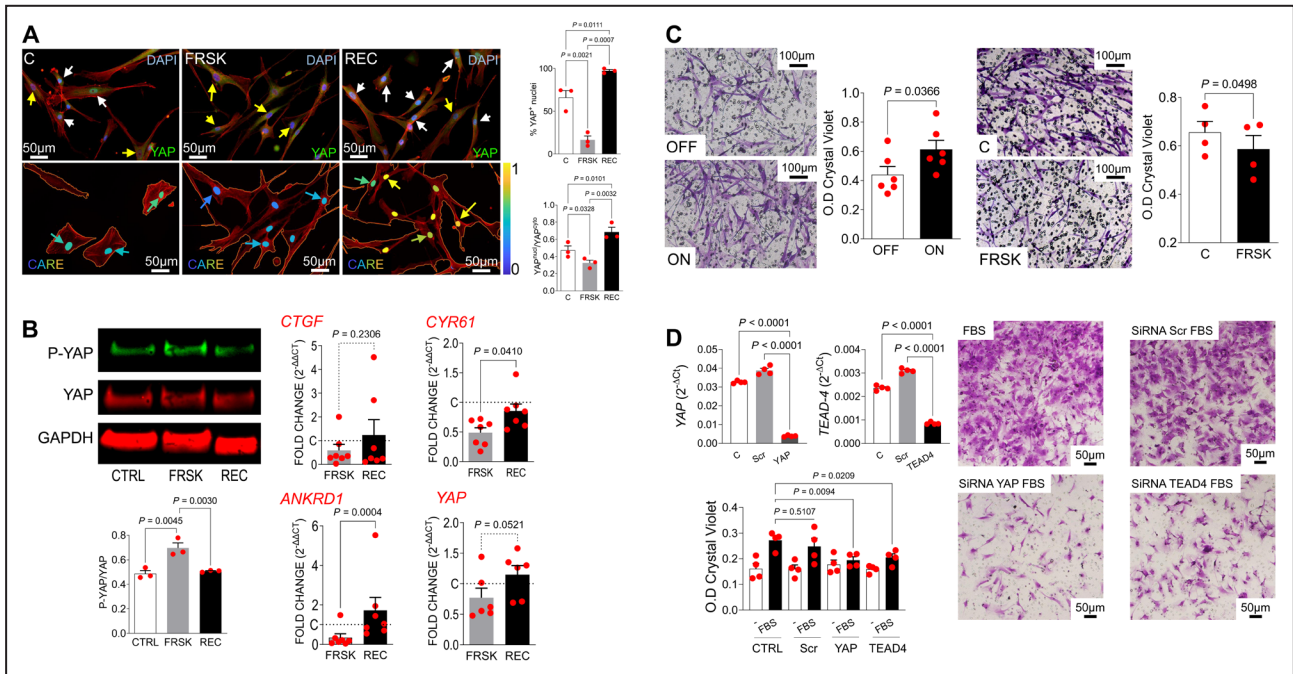


**Figure 2. Dependency of YAP transcriptional activation by cytoskeleton tensing.**

**A**, SVPs plated onto dishes with Mega Pascal mechanical compliance were treated with FRSK, an activator of the adenylate cyclase and the cyclic adenosine monophosphate/ PKA pathway for 6 hours, followed by recovery for an overnight period. The panels on the top show the reversible depolymerization of the F-actin cytoskeleton. White arrows indicate cells with nYAP<sup>+</sup> nuclei, while white arrows show nYAP<sup>-</sup> cells; quantification of these cells is shown in the upper right bar graph. The images on the bottom of the panel show the rendering of the YAP<sup>nuc</sup>/YAP<sup>cyto</sup> ratio as detected by the CARE algorithm. The nuclei of the cells (and the arrows pointing at some of these nuclei) are represented with a different color to discriminate differences in the YAP<sup>nuc</sup>/YAP<sup>cyto</sup> ratio. The color code adopted for this representation is indicated in the bar on the right side of the panels and graphic representation of the YAP<sup>nuc</sup>/YAP<sup>cyto</sup> ratio is included in the lower right bar graph. **B**, Western/ RT-qPCR analyses to detect the effects of FRSK treatment on P-YAP (Ser127) and expression of canonical target genes. As shown in the Western analysis, treatment of SVPs with the PKA activator transiently increased the level of pYAP, consistent with the reversible effect on nuclear localization observed in **(A)**. Inhibition of canonical targets *CTGF*, *CYR61*, and *ANKRD1* also showed a transient inhibition of the YAP transcriptional activity (more pronounced for *CYR61* and *ANKRD1*) and the downregulation of the *YAP* gene itself. **C**, Transwell migration assay of static and dynamically cultured SVPs for 72 hours. As shown in the panels on the left, mechanically stimulated cells (72 hours) migrated more efficiently than those maintained in static culture. Treatment with FRSK inhibited this effect (panel on the right). **D**, Implication of YAP and TEAD in SVPs migration was assessed by siRNA-mediated knockdown experiment. The upper left graphs indicate the downregulation of both transcription factors at a transcriptomic level by RT-qPCR vs the control and scrambled siRNAs. The micrographs on the right show an example of a transwell migration assay performed with control, scrambled siRNA, and YAP/TEAD4 siRNA sequences. As shown, siRNA-mediated downregulation of both transcription factors reduced SVP motility. Quantification of the SVP motility is shown in the bottom bar graph. Data in bar graphs were compared by 1-way ANOVA (repeated-measures) with Tukey (**A**, **B**, **D**; Western blot or RT-qPCR) or Dunnet post hoc tests (**D**, migration), and by paired *t* test in the other graphs. In all graphs, the red dots overlapping the bars indicate the result of each experiment performed in independent cell lines. The *P* values are indicated above the significance lines. CARE indicates Content-Aware Image Restoration; CTRL, control group; DAPI, 4',6-diamidino-2-phenylindole; FBS, fetal bovine serum; FRSK, forskolin; nYAP, nuclear YAP; PKA, protein kinase A; P-YAP, phosphorylated YAP; REC, recovery; RT-qPCR, real-time quantitative polymerase chain reaction; Scr, scrambled small interfering RNA group; siRNA, small interfering RNA; SVP, saphenous vein progenitors; TEAD, TEA domain transcription factor; and YAP, Yes-associated protein.

### Pharmacological Blockade of YAP Reduces Migratory Activity and Fibrotic Differentiation in Response to the TGF-β/TSP-1 Pathway

We previously showed that pharmacological inhibition of YAP by VTP, a Food and Drug Administration-approved inhibitor of the interaction between YAP/TAZ and DNA-binding proteins TEADs,<sup>41</sup> reduces the expression of YAP-dependent targets in human valve interstitial cells<sup>21</sup> and, at least in part, prevents the

mechanical-dependent fibrotic remodeling of the infarcted heart.<sup>20</sup> We therefore assessed the effect of the drug in human SVPs to decrease expression of canonical YAP targets *CTGF*, *CYR61*, and *ANKRD1*. The observed decrease in expression of YAP targets confirmed pharmacological inhibition of YAP by VTP, which was independent of cytoskeleton tensing, as shown by the presence of well-structured stress fibers in VTP-treated samples (Figure S3). In line with existing literature,<sup>42</sup> treatment with VTP also partly inhibited expression of YAP, and reduced the migratory

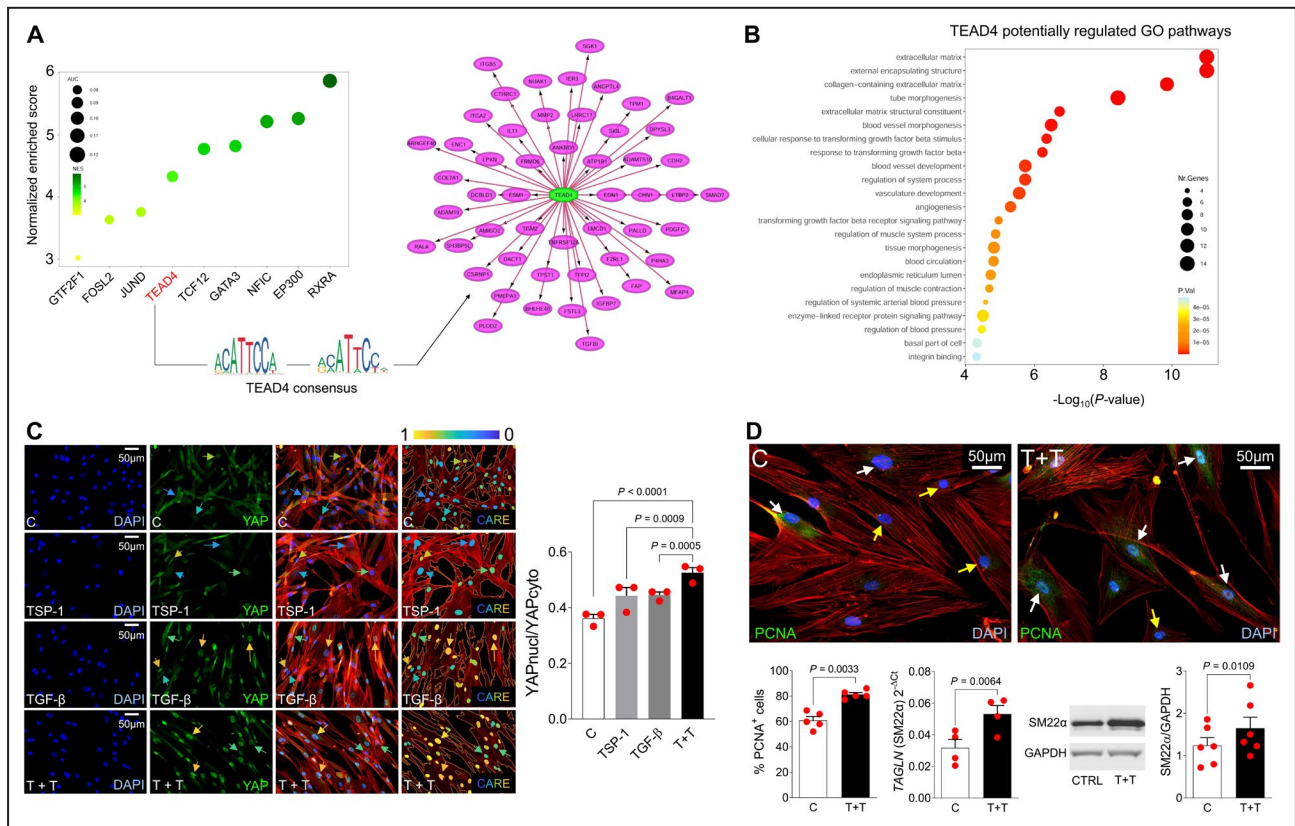


**Figure 3. Cooperation of TEAD 4/ TGF-β transcriptional signaling to mechanoactivation of human SVPs.**  
**A**, Bubble plot of the most represented group of genes contained in their promoter consensus binding sequences of the indicated transcription factors. TEAD4, indicated in red, is one of the most common YAP transcriptional interactors in transcriptional complexes. The gene network represented on the right of the panel indicates the genes that contain the TEAD4 consensus in their promoters and are putatively regulated by YAP/TEAD4 complexes. Note the presence of numerous genes linked to extracellular matrix binding and remodeling, YAP target genes, and genes connected to TGF-β signaling. **B**, Bubble plot representation of an enrichment analysis of the genes containing the 2 TEAD4 consensus binding sequences shown in (A). Among these pathways, again, there was an association of genes to extracellular matrix remodeling and binding and response to TGF-β, suggesting a functional cooperation of the YAP/TEAD4 complex with the TGF-β signaling. **C**, Potentiation of the YAP-dependent signaling by TGF-β and TSP-1. The panels show immunofluorescence staining of SVPs plated onto Mega Pascal substrates in the presence of TGF-β, TSP-1, or a combination of both (T+T). As shown in the immunofluorescence panels, the addition of the single factors enhanced YAP nuclear translocation compared with controls. The T+T combination was, however, the most effective as evidenced by the analysis of the YAP nuclear/cytoplasmic ratio with the CARE algorithm,<sup>34</sup> which indicated a significantly higher YAP<sup>nucl</sup>/YAP<sup>cyto</sup> ratio in cells treated with T+T compared with control or single treatments. As in Figure 2A, the nuclei of the cells (and the arrows pointing at some of these nuclei) are represented with a different color to discriminate differences in the YAP<sup>nucl</sup>/YAP<sup>cyto</sup> ratio. The color code adopted for this representation is indicated in the bar on the top right panels and a graphic representation of the YAP<sup>nucl</sup>/YAP<sup>cyto</sup> ratio is included in the graph on the right. **D**, Stimulation with T+T increased the proliferation of SVPs and the expression (both at the RNA and protein levels) of SM22α early SMC marker. On the top of the panel immunofluorescence shows proliferating cell nuclear antigen (PCNA) as a cell growth marker (note the difference in the number of PCNA<sup>+</sup> cells [white arrows] vs PCNA<sup>-</sup> cells [yellow arrows]), in the T+T compared with control treatment. Quantification of the cells expressing PCNA is represented in the lower left bar graph. Quantification of TAGLN (SM22α) RNA by real-time quantitative polymerase chain reaction and protein by Western analysis was performed to show that treatment with T+T increases SMC differentiation of SVPs. Statistical comparisons were performed by 1-way ANOVA (repeated-measures) with Tukey post hoc in (C) and by paired *t* test in (D). In all graphs, the red dots overlapping the bars indicate the result of each experiment performed in independent cell lines. The *P* values are indicated above the significance lines. CARE indicates Content-Aware Image Restoration; C/CTRL, control group; DAPI, 4',6-diamidino-2-phenylindole; SMC, smooth muscle cell; SVP, saphenous vein progenitors; TEA, TEA domain transcription factor; TGF-β, transforming growth factor β; TSP-1, thrombospondin 1; and YAP, Yes-associated protein.

activity compared with controls (Figure 5A). This reduction coincided with a decrease in the expression of CD47—one of the cellular receptors engaged in SVP migration against TSP-1 gradients,<sup>14</sup> and a

decrease in the number of focal adhesion contacts, as determined by immunofluorescence with anti-vinculin antibodies (Figure 5B). To find a mechanistic link between YAP and TGF-β signaling, we

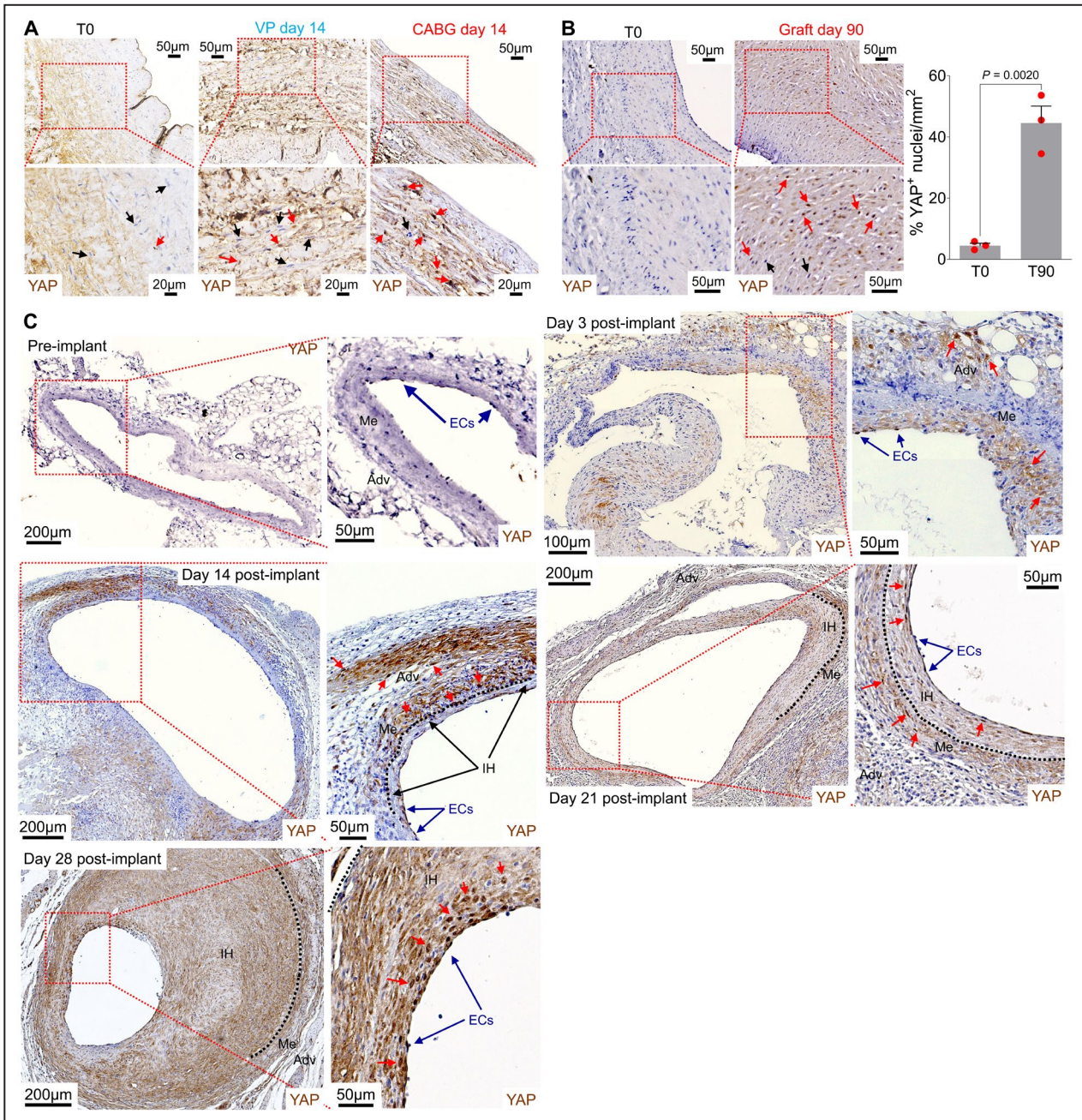


**Figure 4. Dynamics of YAP upregulation in various models of vein arterialization.**

**A**, Exceeding SV conduits recovered from the surgery theater were immediately processed for histology (T0), mounted, and stimulated for 2 weeks in a bioreactor tailored to reproduce a flow with low pressure, typical of the VP, or the counter pulsed coronary circulation, typical of the coronary bypass. Pictures represent transversal sections of the vessels after unmounting from the bioreactors and following histological sectioning and YAP immunohistochemistry. Under these conditions, the cells in CABG-stimulated SVs exhibited a clear upregulation of YAP in the nuclei of the cells in the media (red arrows in the inset). **B**, Transverse sections of pig SVs before and 90 days after implantation into carotids. Evident from the panels in freshly harvested SVs, the expression of YAP was negligible, while at 90 days, several cells in the vein wall were characterized by the presence of the co-factor in the nuclei (red arrows in the inset). Quantification of the cells was performed in 3 independent samples (bar graph on the right). The number of animals included in the quantification is indicated by the red circles overlapping in the bar graph. **C**, The upregulation of YAP in a model of vena cava into carotid interposition in mice was also tested at different times. The images show the transverse section of preimplant and postimplant vena cava immunostained with YAP-specific antibody. It is evident that before implantation, the cells did not express the transcription factor. After implantation, an increasing number of YAP<sup>+</sup> cells were found either in the media (me) or the adventitia (Adv) of the vessel starting at 3 days. Some endothelial cells (ECs; blue arrows) also expressed the factor in line with the role of YAP as a mechanosensor of shear stress.<sup>72</sup> Note the increasing signal of nuclear YAP (red arrows) in cells of the hyperplastic intima (IH) starting at day 21 and culminating at day 28, in keeping with the lumen reduction. The data represented in the bar graph in panel B were compared by unpaired *t* test. The *P* values are indicated above the significance lines. CABG indicates coronary artery bypass graft; SV, saphenous vein; VP, venous perfusion; and Yes-associated protein.

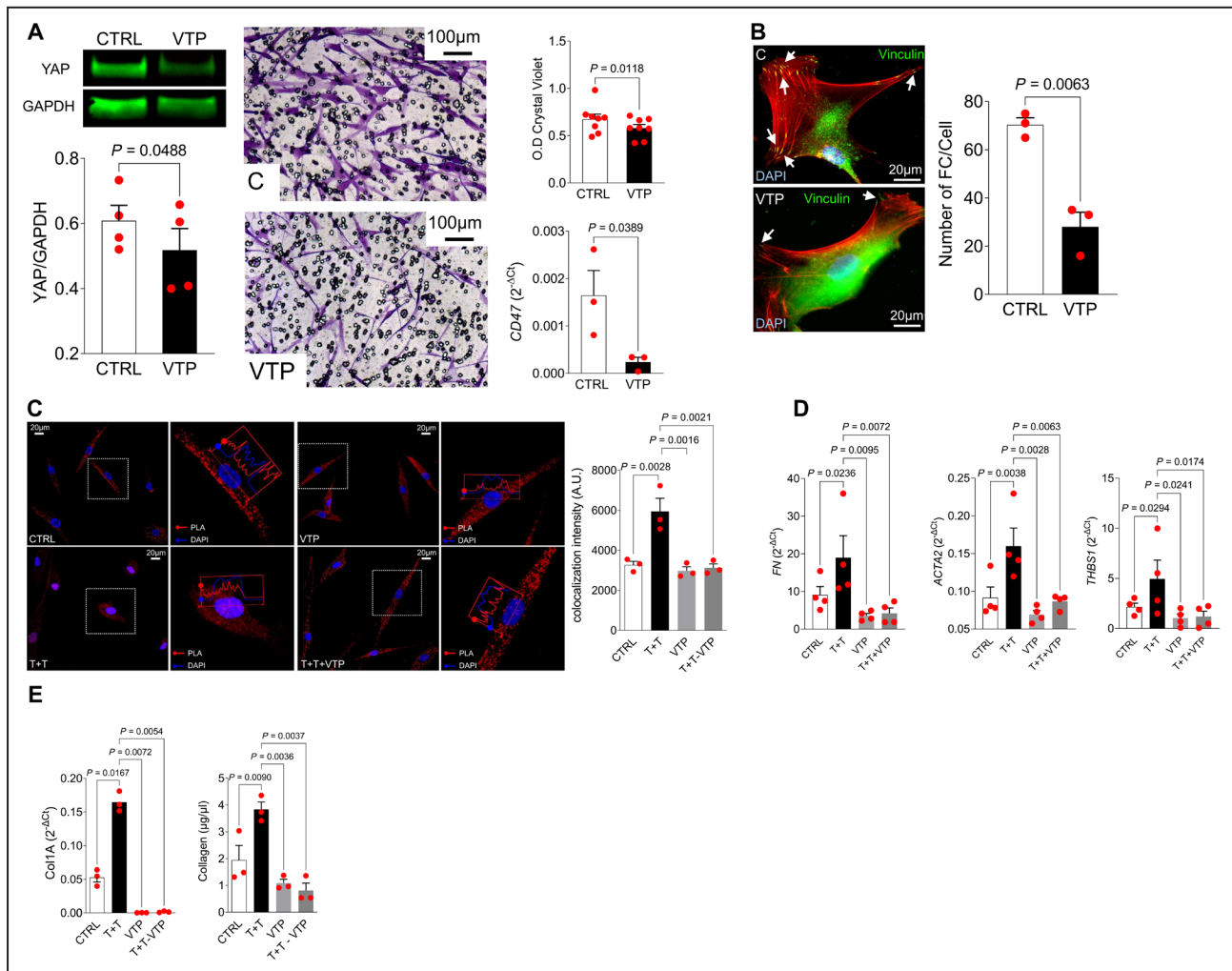


**Figure 5. Interference with YAP transcriptional activity reduces sensitivity to TGF- $\beta$ /TSP-1 signaling.**

**A**, Treating cells with VTP reduces expression of the transcriptional cofactor and migratory activity of human SVPs in transwells. The top left of the panel shows Western blotting analysis of SVPs treated with VTP. Quantification of the Western analysis is shown below. In the center of the panel there is a representative image of the migration assay performed in transwells with control and VTP-treated SVPs; the relative quantification is in the top right. VTP also downregulated expression of CD47, one of the main TSP-1 receptors that have been demonstrated to be relevant for migration of these cells.<sup>14</sup> **B**, VTP reduces the amount of the focal adhesion contacts in SVPs. The left of the panel represents control cells showing a high number of vinculin-stained focal contacts (arrows). VTP significantly inhibited formation of focal contacts/cells, as shown in the bar graph. **C**, PLA performed with YAP and phospho-SMAD3-specific antibodies. The proximity of the 2 transcriptional cofactors was followed by quantifying the red signal in the nuclei of control cells and cells treated with TGF- $\beta$ , TSP-1, and the TGF- $\beta$ /TSP-1 combination (T+T; see the fluorescence profiles overlapping the nuclei of the cells). Evident from the representative images, the red signal was significantly elevated in cells treated with the T+T combination (bar graph on the right). This increase was reverted by VTP, indicating a functional cooperation of TGF- $\beta$  and TSP-1 with nuclear signaling by YAP. **D** through **E**, The TGF- $\beta$ /TSP-1 combination also elevated the RNA expression of key fibrotic/myofibroblasts markers, including fibronectin (*FN*), *ACTA-2* (encoding for  $\alpha$ SMA), and TSP-1 itself (*THBS1*). The combination also elevated the messenger RNA expression and secretion of collagen 1. In all cases, the addition of VTP reduced the expression of these markers to control levels. Statistical comparisons were performed by pairwise Student *t* test in (**A**) and (**B**) and by 1-way ANOVA (repeated-measures) with Tukey post hoc in (**C** through **E**). In all graphs, the red dots overlapping the bars indicate the result of each experiment performed in independent cell lines. The *P* values are indicated above the significance lines. CTRL indicates control group; SVP; saphenous vein progenitors; TGF- $\beta$ , transforming growth factor  $\beta$ ; TSP-1, thrombospondin 1; VTP, verteporfin; and YAP, Yes-associated protein.

hypothesized that YAP directly interacts with SMAD nuclear factors to upregulate expression of genes related to cell proliferation and SMC differentiation.<sup>43</sup> To verify this hypothesis, we first performed a proximity ligation assay (PLA) to assess a possible interaction

of YAP and phospho-SMAD3, and then assessed the expression of various genes and gene products by RT-qPCR and analyzed the cellular supernatants. As shown in Figure 5C, PLA clearly indicated the physical interaction of YAP and phospho-SMAD3 in the

nuclei of cells treated with TGF- $\beta$ /TSP-1 combination, while the presence of VTP reduced the PLA signal to the level of controls, suggesting the direct involvement of YAP in TGF- $\beta$  signaling. RT-qPCR performed on RNA extracted from SVPs showed that several genes relevant to the pathologic progression of VGD<sup>44,45</sup> were upregulated in the presence of the TGF- $\beta$ /TSP-1 combination and were reduced by VTP. This included expression of *FN*, *ACTA-2* ( $\alpha$ SMA), and TSP-1 (*THBS1*) (Figure 5D). Upregulation of collagen—another important effector of fibrosis and VGD progression<sup>46</sup>—was also assessed both at the transcriptional and proteomic level, using RT-qPCR and dosage in cells culture supernatant, respectively (Figure 5E). Moreover, the upregulation of collagen was inhibited by VTP, indicating a direct role of YAP in fibrotic/SMC commitment of SVPs induced by TGF- $\beta$  signaling.

### VTP Improves Vein Graft Remodeling by Inhibiting Intraplaque Angiogenesis and the Fibroproliferative Response In Vivo

To test the therapeutic potential of VTP to improve vein graft remodeling in vivo, hypercholesteremic APOE\*3-Leiden mice underwent venous bypass surgery (Figure 6). Treatment with VTP was initiated at 10 days after surgery—before the upregulation of YAP at 14 days (Figure 4C)—and maintained until euthanasia at day 28 after surgery. VTP treatment was well tolerated, no apparent differences in behavior or wound healing were observed, and body weight was similar between VTP and vehicle (Figure S4). Vein graft remodeling was longitudinally assessed using ultrahigh frequency ultrasound. From 7 days to 28 days, the lumen area was slightly and nonsignificantly increased on VTP treatment compared with a minor decrease in the vehicle group.

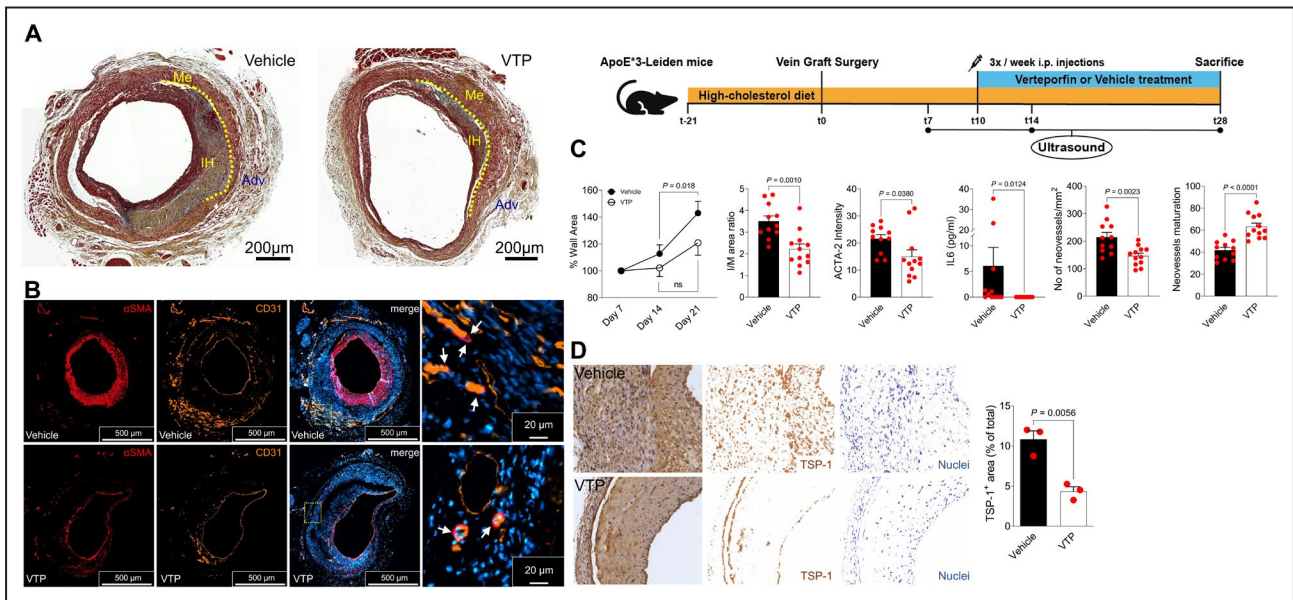


**Figure 6. In vivo administration of VTP blunts progression of vein graft disease in mice.**

**A**, The right side of the panel illustrates the experimental protocol used in our in vivo approach. ApoE\*3-Leiden mice were subjected to a high-fat diet for 21 days before the surgery. After vena cava into carotid interposition, each mouse was monitored by ultrasound at days 7, 10, 14, and 21 after surgery. The intraperitoneal administration of VTP (or vehicle as a control) started at day 10 after surgery. Euthanasia of mice and harvesting of biological material (veins, blood) occurred at day 28 after surgery. The 2 micrographs on the left show a low magnification of the transverse sections of mouse arterialized veins at 28 days postimplant into carotids. Histological sections were stained with Movat pentachrome solution. In mice injected with the control solution (vehicle), the presence of an abundant accumulation of IH and a secondary atherosclerotic plaque is evident, well separated from the preexisting Me. Systemic administration of VTP attenuated intima hyperplasia and, at least in part, reduced the formation of the plaques. **B**, The micrographs show immunofluorescence staining of the veins with antibodies specific for  $\alpha$ SMA (red staining) and CD31 (yellow staining). As shown in the pictures, injection of VTP reduced the number of  $\alpha$ SMA<sup>+</sup> cells in the vein wall and promoted maturation of the neovasculature present in neointima, indicative of reduced atherosclerosis, as shown by the higher number of vessels characterized by coverage of CD31<sup>+</sup> endothelial layer by  $\alpha$ SMA<sup>+</sup> cells (arrows, compare the structure of these vessels in the control vs VTP-treated veins). **C**, Quantification of vessel morphometry (% wall area, I/M ratio),  $\alpha$ SMA (ACTA2) intensity, circulating (pg/mL blood), vessel neoformation (density/mm<sup>2</sup>), and vessel maturation (% of vessels covered by smooth muscle cells). **D**, VTP significantly reduces the expression of TSP-1. The micrographs indicate the immunohistochemistry of the explanted vein grafts in control and VTP-injected mice. It is evident the reduction in the positive area in treated mice compared with controls (quantification in the bar graph on the right). Data in the bar graphs were compared by unpaired *t* test. In all graphs, the red dots overlapping the bars indicate the result of each experiment performed in independent animals. The *P* values are indicated above the significance lines. IL6 indicates interleukin 6; I/M, intima/media; IH, intimal; Me, media; TSP, thrombospondin 1; and VTP, vertepofrin.

In addition, the wall area increased significantly during the same period, and this was in part inhibited by VTP (Figure 6C). In-depth analysis of the vessel wall on histology revealed that VTP determined a reduction in the ratio between the areas occupied by the intima and the media in the transversal sections (intima/media ratio), indicating improved vein graft remodeling (Figure 6A and 6C). To evaluate whether VTP affected plaque stability, cellular compositional analysis on the vein grafts was performed. In line with our *in vitro* results, expression of ACTA2 ( $\alpha$ SMA) was decreased by VTP (Figure 6B and 6C). Due to the critical role of YAP in endothelial cells, we finally explored whether VTP inhibited intraplaque angiogenesis, a hallmark of unstable atherosclerotic plaques. Plaque angiogenesis is rarely observed in naïve murine atherosclerosis; however, it is a unique feature observed in our atherosclerotic vein graft model.<sup>47</sup> The number of neovessels per mm<sup>2</sup> was significantly reduced by VTP compared with vehicle. Moreover, VTP increased ACTA2 coverage of these neovessels, indicating improved neovessel maturation (Figure 6B and 6C). Finally, given the involvement of TSP-1 in SV mechanical-dependent arterialization,<sup>14</sup> we quantified the TSP-1<sup>+</sup> vein graft area. Vein grafts of VTP-treated mice exhibited significantly less staining, indicating a reduction in the expression of the matricellular protein, in line with *in vitro* results (Figures 6D), and, consequently, intragraft TGF- $\beta$  signaling. VTP also reduced systemic interleukin 6 levels, indicative of less systemic inflammation<sup>48</sup> and, hence, reduced pathological vein graft remodeling.

## DISCUSSION

The problem of maladaptive remodeling in venous coronary artery bypasses has been recognized since the first follow-up studies in the early 1970s.<sup>49</sup> Since then, it was hypothesized that the damage caused during graft harvesting/preparation and the subsequent exposure to an unphysiological flow/pressure regimen is one of the major causes of the remodeling, in cooperation with other important factors such as inflammation, hypercholesterolemia, and hypertension.<sup>5</sup> While various strategies have been implemented to improve vein graft patency, such as the adoption of external stenting,<sup>50</sup> the use of “no-touch” harvesting procedures,<sup>51</sup> and the storage of vessels in protective buffers during extracorporeal exposure,<sup>52</sup> the progressive occlusion of venous grafts remains a major challenge, exposing patients to recurrence of ischemia.<sup>53</sup>

Various studies have been conducted to identify the cellular and molecular determinants of vein graft failure, leading to the identification and validation of key players such as metalloproteases and cell cycle genes in animal models, using approaches such as gene therapy.<sup>11,54</sup> Some of the most promising results, at least in preclinical models, were obtained with the

transfer of TIMP-3 (tissue inhibitor of metalloproteinases-3),<sup>55</sup> p53 (tumor protein p53),<sup>56</sup> and endothelial nitric oxide synthase<sup>57</sup> genes. By contrast, the only clinical trial performed to date, the PREVENT (Prevention of Restenosis After Vascular Intervention) trial,<sup>58</sup> based on treating the grafts with E2F decoy edifoligide, has not met expectations in terms of disease reduction.<sup>59,60</sup> Other interesting targets such as miR-21<sup>61</sup> or inflammatory mediators (eg, MCP-1 [monocyte chemoattractant protein-1]/CCL2 [C-C motif ligand 2] chemokine<sup>62</sup> and Toll-like receptors<sup>63</sup>) have been identified in preclinical studies, but their significance has not yet been fully established.

## Involvement of a YAP/TGF- $\beta$ Signaling Network in Mechanical Pathologic Programming of SVPs

The saphenous conduits are living vessels that are removed from their natural bed to bypass the obstructions present in the coronary tree. Apart from endothelial cells, which are important for vascular permeability, and SMCs, which are important for the maintenance of vascular tone, other cell types are present in the intact vessel structure. SVPs are normally associated with vasa vasorum, from which they can be isolated as CD34<sup>+</sup>/NG2<sup>+</sup>/CD31<sup>-</sup> cells.<sup>16</sup> While the main function of these cells is to maintain vascular homeostasis, their potential pathogenetic role has also been highlighted, with evidence that they can be activated and give rise to fibrotic cells undergoing epigenetic modifications.<sup>15</sup> Using bioreactors tailored to expose human SVs to pressure or flow/pressure regimens typical of coronary circulation, we have shown in various publications that the pulsatile stress to which the SV grafts are subjected during arterialization causes extensive morphological remodeling and activates TGF- $\beta$ -dependent signaling mediated by TSP-1; this matricellular factor is likely involved in the recruitment of adventitial progenitors.<sup>13,14,64,65</sup> In the present study, we aimed to contextualize the effects of mechanical forces on the pathologic programming of these cells when exposed to uniaxial strain (10% elongation) cyclic stimulation. This condition accurately corresponds to the mechanical solicitation that cells experience in the SV wall, according to a numerical model of the radial strain associated with the counter pulsed coronary flow in the grafts.<sup>14</sup> By whole genome transcriptomics and bioinformatics, we found numerous differentially expressed genes and obtained a clear indication of transcriptional networks that may be involved in cell/extracellular matrix interactions, proliferation, and crosstalk with the TGF- $\beta$  signaling (Figure 1). We also assessed whether, similar to cardiac fibroblasts,<sup>20,26</sup> the mechanical sensing of SVPs involved the participation of components of the so-called Hippo

transcriptional pathway.<sup>18</sup> Particular care was dedicated to assess a functional convergence of YAP (the most investigated Hippo transcriptional co-factor) with nuclear signaling downstream of TGF- $\beta$  and the relationship with TEADs, the canonical cognate DNA-binding proteins of the YAP/TAZ complex.<sup>66,67</sup> Our results clearly indicated mechanical-dependent modulation of genes represented as canonical YAP targets (*CTGF*, *CYR61*, and *ANKRD1*) and encoding for TGF- $\beta$  transcriptional effectors (*SMAD2/7*) (Figure 1D and 1G). This regulation likely involved the F-actin cytoskeleton, as demonstrated by the reversible downregulation of the YAP targets by treating SVPs with FRSK, an activator of the cyclic adenosine monophosphate/protein kinase A pathway (Figure 2A and 2B),<sup>32,68</sup> and the cooperation of TEAD4 as a transcriptional co-factor, as assessed by bioinformatics (Figure 3A and 3B). The role of YAP in myofibroblast differentiation of human SVPs was further contextualized in the light of our previous findings showing that mechanical strain amplifies the effects of TGF- $\beta$  through the release of TSP-1 from SMCs of the SV, as a result of a contractile to secretory phenotype switch.<sup>14</sup> In particular, the combination of soluble TSP-1 and TGF- $\beta$  enhanced the YAP nuclear signaling compared with the single treatments (Figure 3C), and this increased cellular proliferation and expression of SM22 $\alpha$  (Figure 3D), ACTA2, FN, TSP1, collagen 1 (Figure 5D and 5E), and, finally, the physical association with phospho-SMAD3 in the nuclei of the treated cells (Figure 5C). In line with findings from other groups in different model systems showing cooperation of YAP with components of TGF- $\beta$  signaling (in particular SMAD2/3 nuclear proteins) in endothelial-mesenchymal transition,<sup>69</sup> or arterial stiffening,<sup>70</sup> our data consolidate the role of YAP as a transcriptional co-factor with crucial roles in the integration of mechanical and fibrotic signaling in cardiovascular pathologies.<sup>71</sup>

### In Vivo Blockade of YAP Reduces VGD

On the basis of our previous findings suggesting that YAP is involved in strain-dependent activation of cardiac fibroblasts in the ischemic heart,<sup>20</sup> we investigated the expression of the transcriptional co-factor in 3 independent models of vein arterialization (Figure 4). In the first model, using a bioreactor capable of mimicking the flow and pressure patterns typical of coronary circulation,<sup>13,14</sup> we performed arterialization of ex vivo human SV segments for up to 14 days. In a second approach, we used a gold-standard large animal model of bypass failure by interposing the SV into the carotid arteries of pigs, with a 90-day follow-up.<sup>40</sup> Finally, we performed a mouse model of vena cava into carotid interposition in hypercholesterolemic mice, with a follow-up to 28 days.<sup>23</sup> Although with different dynamics

and efficiency, in all of these models, the localization of YAP in the nuclei of cells in the medial layer increased. Remarkably, as shown in the panels in Figure 4, the nuclear localization of the factor was pronounced in the endothelial cells lining the lumen<sup>72</sup> and in the cells that had an elongated nuclear shape. This pattern was similar to what we previously observed in the mouse hearts, where the fibroblasts were exposed to compression forces generated by the distribution of the radial strain.<sup>20</sup> We then aimed to modulate YAP signaling in vivo and reduce the molecular translation of the mechanical cues. To achieve this aim we employed transplantation of the vena cava into the carotids of hypercholesterolemic mice<sup>23</sup> and administered VTP, a drug that can be used in nonphotodynamic inhibition of the YAP/TAZ/TEADs complexes transcriptional function.<sup>41,73</sup> Longitudinal follow-up of vein graft remodeling using ultrahigh frequency ultrasound clearly showed a stepwise increase in the wall area and this, as shown in Figure 6, involved extensive intima hyperplasia in control animals. Interestingly, these zones were the ones in which the cells expressed high levels of  $\alpha$ SMA (Figure 6B) and TSP-1 (Figure 6D), consistent with a myofibroblast and secretory phenotype. Administration of VTP reduced this stepwise increase and prevented accumulation of  $\alpha$ SMA<sup>+</sup> cells in the subintimal layer. This was accompanied by remarkable inhibition of the vessel wall remodeling (as assessed by reduction of the intima/media ratio), and of the area of the vein wall containing TSP-1<sup>+</sup> cells (Figure 6C and 6D). Finally, VTP treatment also drastically reduced the presence of interleukin 6 in peripheral blood, suggestive of reduced inflammation,<sup>74,75</sup> and suppressed intraplaque angiogenesis, while concomitantly enhancing the maturation of these newly formed vessels, thus improving plaque stability.<sup>47,76,77</sup> This warrants pharmacological YAP targeting as a new strategy to reduce the myofibroblastic response and adverse vein graft remodeling in less exploratory and more preclinically oriented studies.

### CONCLUSIONS

During coronary transplantation, the cells residing in the wall of the SV grafts (eg, preexisting ECs, SMCs, and SVPs) are subjected to a sudden increase of mechanical forces, including shear stress and longitudinal and transversal wall strain.<sup>78</sup> These forces have been mechanistically connected to the progression of VGD. For example, we have found that exposure of human SVs to a wall strain typical of the coronary-like flow/pressure pattern triggers a fibrotic process mediated by TGF- $\beta$ /TSP-1 signaling.<sup>14,65</sup> In the current study, we show that mechanical signaling induces a fibrotic evolution of SVPs involving the differential expression of several gene pathways connected to extracellular

matrix remodeling and cellular/matrix interactions. Our data also suggest that there is a synergistic effect of mechanical forces and matricellular signaling elicited by the TGF- $\beta$ /TSP-1 combination. This was shown by a drastic increase in SMC/fibrotic marker (*FN*, *ACTA-2*, *TSP-1*, *Collagen*) expression when SVPs were treated with a combination of the 2 fibrotic factors onto rigid substrates, and by the crucial role of YAP as a mechanically activated transcriptional co-factor in their phenotypic transformation.

The recent preclinical success of external stenting to reduce the impact of the unphysiological wall mechanics to consequently reduce adverse vein graft remodeling, highlights that limiting transmission of the excess strain is crucial in reducing excessive cell proliferation and, hence, delay bypass failure.<sup>79,80</sup> This protective effect is mediated through modulation of YAP signaling<sup>81</sup> and provides compelling evidence for the so-called “mechanotherapeutic” approach as a new avenue to prevent maladaptive remodeling of cardiovascular tissues.<sup>71</sup> Our results indicate that this approach is practicable, even though particular care will have to be dedicated to choose an appropriate release system of the drug locally to the graft.

In summary, our findings suggest that reducing mechanically induced activation of vein resident progenitors by pharmacologically targeting YAP could have beneficial effects on reducing intima hyperplasia by targeting vein resident progenitors as precursors of activated fibroblasts and, potentially, SMCs. While this is a potentially different approach compared with gene therapy that has been historically employed to target SMCs hyperplasia,<sup>82</sup> it also provides new opportunities for the development of new devices such as nanotechnologies or materials endowed with a slow-release drug potential to maximize therapeutic effects. Various options are available such as pretreating the grafts with the drug before being reimplanted in the patient (such as in existing gene therapy trials) or to release the drug by active or passive support systems (eg, nanoparticles, drug-releasing external stents, drug-containing hydrogels).<sup>83</sup> We anticipate that these strategies might be helpful to minimize the side effects of systemic drug administration and localize the therapeutic intervention to the grafts.

## Study Limitations

The present investigation is a proof-of-concept study that inhibition of YAP with VTP may be effective in preventing the maladaptive remodeling of the arterialized vein caused by the sensing of mechanical forces. Although, in line with our previous findings in the infarcted heart,<sup>20</sup> this effect was mechanistically related to the reduction of the TGF- $\beta$ -dependent transcriptional pathways in cultured SVPs, the inhibition of vascular remodeling in vivo could be caused

by the cumulation of unrelated effects such as inhibition of inflammation,<sup>84</sup> inhibition of proliferation and enhancement of apoptosis,<sup>85</sup> or a reduction in oxidative phosphorylation activity.<sup>86</sup> More targeted, cell-specific approaches for YAP inhibition should be investigated in the future to address this important mechanistic point.

Another limitation of the present study is the modality of VTP administration in the animal model of vein graft administration. We are aware of the disadvantages that systemic injection of the drug may cause, given its pleiotropic action. In this regard, we anticipate that exposure of the SV to the drug or mixing the drug with a polymer that could be used to slowly release it on the adventitial side might increase the efficiency of the treatment and minimize the side effects. This feasibility of the last option has been shown in the literature<sup>81</sup> and we are presently implementing systems to pursue it.

## ARTICLE INFORMATION

Received July 6, 2024; accepted January 28, 2025.

### Affiliations

Centro Cardiologico Monzino, IRCCS, Milan, Italy (G.G., L.P., M.S.R., A.S., C.S., S.Z., M.C., M.A., M.P.); Einthoven Laboratory for Experimental Vascular Medicine, Department of Surgery, Leiden University Medical Center (LUMC), Leiden, The Netherlands (T.J.S., T.Y., P.H.Q., M.R.d.V.); Bristol Medical School, University of Bristol, United Kingdom (A.T., P.M.); Dipartimento di Ingegneria Meccanica e Aerospaziale, Politecnico di Torino, Turin, Italy (M.S., F.M., U.M., M.P.); Dipartimento di Bioingegneria, Elettronica ed Informazione, Politecnico di Milano, Milan, Italy (M.S., G.B.F.); Laboratorio di Cardiologia Molecolare, IRCCS Policlinico San Donato, Milan, Italy (F.M.); Humanitas Cardio-Center, IRCCS Humanitas Research Hospital, Rozzano, Italy (G.C.); Department of Biomedical Sciences, Humanitas University, Pieve Emanuele, Italy (G.C.); Unità di Ricerca Cardiovascolare, IRCCS Multimedica, Milan, Italy (G.S.); Department of Surgery, Brigham & Women's Hospital and Harvard Medical School, Boston, MA (M.R.d.V.); and Department of Cell Biology, King Faisal Specialist Hospital & Research Center, Riyadh, Saudi Arabia (M.P.).

### Sources of Funding

The present research was granted by institutional research funding issued by the Italian Ministry of Health (Ricerca Corrente, project numbers 2764157, 2771985, 2775037) to M.P. F.M. is supported by the Italian Ministry of Health (“Ricerca Corrente 2023”, RF-2019-12368521, POS T4 CAL.HUB.RIA, cod. T4-AN-09), by Telethon Foundation (#4462 GGP19035A), AFM Rialto (# 23054), and by the EU-Next Generation EU-NRRP M6C2 – Inv.2.1 PNRR-MAD-2022-12375790. M.d.V. was supported by a grant funded by the Rembrandt Institute for Cardiovascular Science.

### Disclosures

None.

### Supplemental Material

Data S1  
Tables S1–S3  
Figures S1–S4  
Data sets S1–S5  
References [87–96]  
Data S2

## REFERENCES

- Gaudio M, Benedetto U, Fremez S, Ballman K, Biondi-Zoccai G, Sedrakyan A, Nasso G, Raman J, Buxton B, Hayward PA, et al. Association of radial artery graft vs saphenous vein graft with

- long-term cardiovascular outcomes among patients undergoing coronary artery bypass grafting. *JAMA*. 2020;324:179–187. doi: [10.1001/jama.2020.8228](https://doi.org/10.1001/jama.2020.8228)
2. Xenogiannis I, Zenati M, Bhatt DL, Rao SV, Rodes-Cabau J, Goldman S, Shunk KA, Mavromatis K, Banerjee S, Alaswad K, et al. Saphenous vein graft failure: from pathophysiology to prevention and treatment strategies. *Circulation*. 2021;144:728–745. doi: [10.1161/CIRCULATIONAHA.120.052163](https://doi.org/10.1161/CIRCULATIONAHA.120.052163)
  3. Arsalan M, Mack MJ. Coronary artery bypass grafting is currently underutilized. *Circulation*. 2016;133:1036–1045. doi: [10.1161/CIRCULATIONAHA.115.018032](https://doi.org/10.1161/CIRCULATIONAHA.115.018032)
  4. Farber A, Menard MT, Conte MS, Kaufman JA, Powell RJ, Choudhry NK, Hamza TH, Assmann SF, Creager MA, Cziraky MJ, et al. Surgery or endovascular therapy for chronic limb-threatening ischemia. *N Engl J Med*. 2022;387:2305–2316. doi: [10.1056/NEJMoa2207899](https://doi.org/10.1056/NEJMoa2207899)
  5. Caliskan E, de Souza DR, Boning A, Liakopoulos OJ, Choi YH, Pepper J, Gibson CM, Perrault LP, Wolf RK, Kim KB, et al. Saphenous vein grafts in contemporary coronary artery bypass graft surgery. *Nat Rev Cardiol*. 2020;17:155–169. doi: [10.1038/s41569-019-0249-3](https://doi.org/10.1038/s41569-019-0249-3)
  6. de Vries MR, Quax PHA. Inflammation in vein graft disease. *Front Cardiovasc Med*. 2018;5. doi: [10.3389/fcvm.2018.00003](https://doi.org/10.3389/fcvm.2018.00003)
  7. de Vries MR, Simons KH, Jukema JW, Braun J, Quax PHA. Vein graft failure: from pathophysiology to clinical outcomes. *Nat Rev Cardiol*. 2016;13:451–470. doi: [10.1038/nrcardio.2016.76](https://doi.org/10.1038/nrcardio.2016.76)
  8. Hu Y, Xu Q. Adventitial biology: differentiation and function. *Arterioscler Thromb Vasc Biol*. 2011;31:1523–1529. doi: [10.1161/atvbaha.110.221176](https://doi.org/10.1161/atvbaha.110.221176)
  9. Torsney E, Hu Y, Xu Q. Adventitial progenitor cells contribute to arteriosclerosis. *Trends Cardiovasc Med*. 2005;15:64–68. doi: [10.1016/j.tcm.2005.02.003](https://doi.org/10.1016/j.tcm.2005.02.003)
  10. Hu Y, Zhang Z, Torsney E, Afzal AR, Davison F, Metzler B, Xu Q. Abundant progenitor cells in the adventitia contribute to atherosclerosis of vein grafts in ApoE-deficient mice. *J Clin Invest*. 2004;113:1258–1265. doi: [10.1172/jci19628](https://doi.org/10.1172/jci19628)
  11. Southerland KW, Frazier SB, Bowles DE, Milano CA, Kontos CD. Gene therapy for the prevention of vein graft disease. *Transl Res*. 2013;161:321–338. doi: [10.1016/j.trsl.2012.12.003](https://doi.org/10.1016/j.trsl.2012.12.003)
  12. Newby AC. Coronary vein grafting: the flags keep waving but the game goes on. *Cardiovasc Res*. 2013;97:193–194. doi: [10.1093/cvr/cvs351](https://doi.org/10.1093/cvr/cvs351)
  13. Piola M, Ruiter M, Vismara R, Mastrullo V, Agrifoglio M, Zanobini M, Pesce M, Soncini M, Fiore GB. Full mimicking of coronary hemodynamics for ex-vivo stimulation of human saphenous veins. *Ann Biomed Eng*. 2017;45:884–897. doi: [10.1007/s10439-016-1747-7](https://doi.org/10.1007/s10439-016-1747-7)
  14. Garoffolo G, Ruiter MS, Piola M, Brioschi M, Thomas AC, Agrifoglio M, Polvani G, Coppadoro L, Zoli S, Saccu C, et al. Coronary artery mechanics induces human saphenous vein remodeling via recruitment of adventitial myofibroblast-like cells mediated by thrombospondin-1. *Theranostics*. 2020;10:2597–2611. doi: [10.7150/thno.40595](https://doi.org/10.7150/thno.40595)
  15. Gubernator M, Slater SC, Spencer HL, Spiteri I, Sottoriva A, Riu F, Rowlinson J, Avolio E, Katare R, Mangialardi G, et al. Epigenetic profile of human adventitial progenitor cells correlates with therapeutic outcomes in a mouse model of limb ischemia. *Arterioscler Thromb Vasc Biol*. 2015;35:675–688. doi: [10.1161/atvbaha.114.304989](https://doi.org/10.1161/atvbaha.114.304989)
  16. Campagnolo P, Cesselli D, Al Haj Zen A, Beltrami AP, Kränkel N, Katare R, Angelini G, Emanuelli C, Madeddu P. Human adult vena saphena contains perivascular progenitor cells endowed with clonogenic and proangiogenic potential. *Circulation*. 2010;121:1735–1745. doi: [10.1161/circulationaha.109.899252](https://doi.org/10.1161/circulationaha.109.899252)
  17. Dupont S, Morsut L, Aragona M, Enzo E, Giulitti S, Cordenonsi M, Zanonato F, Le Digabel J, Forcato M, Bicciato S, et al. Role of YAP/TAZ in mechanotransduction. *Nature*. 2011;474:179–183. doi: [10.1038/nature10137](https://doi.org/10.1038/nature10137)
  18. Piccolo S, Dupont S, Cordenonsi M. The biology of YAP/TAZ: hippo signaling and beyond. *Physiol Rev*. 2014;94:1287–1312. doi: [10.1152/physrev.00005.2014](https://doi.org/10.1152/physrev.00005.2014)
  19. Schroer AK, Merryman WD. Mechanobiology of myofibroblast adhesion in fibrotic cardiac disease. *J Cell Sci*. 2015;128:1865–1875. doi: [10.1242/jcs.162891](https://doi.org/10.1242/jcs.162891)
  20. Garoffolo G, Casaburo M, Amadeo F, Salvi M, Bernava G, Piacentini L, Chimenti I, Zaccagnini G, Milcovich G, Zuccolo E, et al. Reduction of cardiac fibrosis by interference with YAP-dependent transactivation. *Circ Res*. 2022;131:239–257. doi: [10.1161/CIRCRESAHA.121.319373](https://doi.org/10.1161/CIRCRESAHA.121.319373)
  21. Santoro R, Scaini D, Severino LU, Amadeo F, Ferrari S, Bernava G, Garoffolo G, Agrifoglio M, Casalis L, Pesce M. Activation of human aortic valve interstitial cells by local stiffness involves YAP-dependent transcriptional signaling. *Biomaterials*. 2018;181:268–279. doi: [10.1016/j.biomaterials.2018.07.033](https://doi.org/10.1016/j.biomaterials.2018.07.033)
  22. Nardone G, La Cruz JOD, Vrbsky J, Martini C, Pribyl J, Skladal P, Pestl M, Caluori G, Pagliari S, Martino F, et al. YAP regulates cell mechanics by controlling focal adhesion assembly. *Nat Commun*. 2017;8:15321. doi: [10.1038/Ncomms15321](https://doi.org/10.1038/Ncomms15321)
  23. Lardenoye JH, de Vries MR, Lowik CW, Xu Q, Dhore CR, Cleutjens JP, van Hinsbergh VW, van Bockel JH, Quax PH. Accelerated atherosclerosis and calcification in vein grafts: a study in APOE<sup>3</sup> Leiden transgenic mice. *Circ Res*. 2002;91:577–584. doi: [10.1161/01.res.0000036901.58329.d7](https://doi.org/10.1161/01.res.0000036901.58329.d7)
  24. Thomas AC, Wyatt MJ, Newby AC. Reduction of early vein graft thrombosis by tissue plasminogen activator gene transfer. *Thromb Haemost*. 2009;102:145–152. doi: [10.1160/TH08-11-0772](https://doi.org/10.1160/TH08-11-0772)
  25. Maselli D, Garoffolo G, Cassanmagnago GA, Vono R, Ruiter MS, Thomas AC, Madeddu P, Pesce M, Spinetti G. Mechanical strain induces transcriptomic reprogramming of saphenous vein progenitors. *Front Cardiovasc Med*. 2022;9:884031. doi: [10.3389/fcvm.2022.884031](https://doi.org/10.3389/fcvm.2022.884031)
  26. Ugolini GS, Rasponi M, Pavesi A, Santoro R, Kamm R, Fiore GB, Pesce M, Soncini M. On-chip assessment of human primary cardiac fibroblasts proliferative responses to uniaxial cyclic mechanical strain. *Biotechnol Bioeng*. 2016;113:859–869. doi: [10.1002/bit.25847](https://doi.org/10.1002/bit.25847)
  27. Piersma B, Bank RA, Boersema M. Signaling in fibrosis: TGF-beta, WNT, and YAP/TAZ converge. *Front Med (Lausanne)*. 2015;2:59. doi: [10.3389/fmed.2015.00059](https://doi.org/10.3389/fmed.2015.00059)
  28. Zhao B, Wei X, Li W, Udan RS, Yang Q, Kim J, Xie J, Ikenoue T, Yu J, Li L, et al. Inactivation of YAP oncoprotein by the hippo pathway is involved in cell contact inhibition and tissue growth control. *Genes Dev*. 2007;21:2747–2761. doi: [10.1101/gad.1602907](https://doi.org/10.1101/gad.1602907)
  29. Aragona M, Panciera T, Manfrin A, Giulitti S, Michielin F, Elvassore N, Dupont S, Piccolo S. A mechanical checkpoint controls multicellular growth through YAP/TAZ regulation by actin-processing factors. *Cell*. 2013;154:1047–1059. doi: [10.1016/j.cell.2013.07.042](https://doi.org/10.1016/j.cell.2013.07.042)
  30. Xiao Y, Hill MC, Li L, Deshmukh V, Martin TJ, Wang J, Martin JF. Hippo pathway deletion in adult resting cardiac fibroblasts initiates a cell state transition with spontaneous and self-sustaining fibrosis. *Genes Dev*. 2019;33:1491–1505. doi: [10.1101/gad.329763.119](https://doi.org/10.1101/gad.329763.119)
  31. Dey A, Varelas X, Guan KL. Targeting the hippo pathway in cancer, fibrosis, wound healing and regenerative medicine. *Nat Rev Drug Discov*. 2020;19:480–494. doi: [10.1038/s41573-020-0070-z](https://doi.org/10.1038/s41573-020-0070-z)
  32. Kimura TE, Duggirala A, Smith MC, White S, Sala-Newby GB, Newby AC, Bond M. The hippo pathway mediates inhibition of vascular smooth muscle cell proliferation by cAMP. *J Mol Cell Cardiol*. 2016;90:1–10. doi: [10.1016/j.yjmcc.2015.11.024](https://doi.org/10.1016/j.yjmcc.2015.11.024)
  33. Howe AK. Regulation of actin-based cell migration by cAMP/PKA. *Biochim Biophys Acta*. 2004;1692:159–174. doi: [10.1016/j.bbamer.2004.03.005](https://doi.org/10.1016/j.bbamer.2004.03.005)
  34. Salvi M, Morbiducci U, Amadeo F, Santoro R, Angelini F, Chimenti I, Massai D, Messina E, Giacomello A, Pesce M, et al. Automated segmentation of fluorescence microscopy images for 3D cell detection in human-derived Cardiospheres. *Sci Rep*. 2019;9:6644. doi: [10.1038/s41598-019-43137-2](https://doi.org/10.1038/s41598-019-43137-2)
  35. Mana-Capelli S, McCollum D. Angiomotins stimulate LATS kinase autophosphorylation and act as scaffolds that promote hippo signaling. *J Biol Chem*. 2018;293:18230–18241. doi: [10.1074/jbc.RA118.004187](https://doi.org/10.1074/jbc.RA118.004187)
  36. Chen Y, Zhao X, Sun J, Su W, Zhang L, Li Y, Liu Y, Zhang L, Lu Y, Shan H, et al. YAP1/twist promotes fibroblast activation and lung fibrosis that conferred by miR-15a loss in IPF. *Cell Death Differ*. 2019;26:1832–1844. doi: [10.1038/s41418-018-0250-0](https://doi.org/10.1038/s41418-018-0250-0)
  37. Fujii M, Toyoda T, Nakanishi H, Yatabe Y, Sato A, Matsudaira Y, Ito H, Murakami H, Kondo Y, Kondo E, et al. TGF-β synergizes with defects in the hippo pathway to stimulate human malignant mesothelioma growth. *J Exp Med*. 2012;209:479–494. doi: [10.1084/jem.20111653](https://doi.org/10.1084/jem.20111653)
  38. Ebrahimighaei R, Sala-Newby GB, Hudson C, Kimura TE, Hathway T, Hawkins J, McNeill MC, Richardson R, Newby AC, Bond M. Combined role for YAP-TEAD and YAP-RUNX2 signalling in substrate-stiffness regulation of cardiac fibroblast proliferation. *Biochim Biophys Acta Mol Cell Res*. 2022;1869:119329. doi: [10.1016/j.bbamer.2022.119329](https://doi.org/10.1016/j.bbamer.2022.119329)
  39. Humeres C, Venugopal H, Frangogiannis NG. Smad-dependent pathways in the infarcted and failing heart. *Curr Opin Pharmacol*. 2022;64:102207. doi: [10.1016/j.coph.2022.102207](https://doi.org/10.1016/j.coph.2022.102207)
  40. Thomas AC. Animal models for studying vein graft failure and therapeutic interventions. *Curr Opin Pharmacol*. 2012;12:121–126. doi: [10.1016/j.coph.2012.01.002](https://doi.org/10.1016/j.coph.2012.01.002)

41. Gibault F, Corvaisier M, Bailly F, Huet G, Melnyk P, Cotelle P. Non-Photoinduced biological properties of Verteporfin. *Curr Med Chem*. 2016;23:1171–1184. doi: [10.2174/0929867323666160316125048](https://doi.org/10.2174/0929867323666160316125048)
42. Wei L, Ma X, Hou Y, Zhao T, Sun R, Qiu C, Liu Y, Qiu Z, Liu Z, Jiang J. Verteporfin reverses progesterin resistance through YAP/TAZ-PI3K-Akt pathway in endometrial carcinoma. *Cell Death Dis*. 2023;9. doi: [10.1038/s41420-023-01319-y](https://doi.org/10.1038/s41420-023-01319-y)
43. Szeto SG, Narimatsu M, Lu M, He X, Sidiqi AM, Tolosa MF, Chan L, De Freitas K, Bialik JF, Majumder S, et al. YAP/TAZ are mechanoregulators of TGF- $\beta$ -Smad signaling and renal fibrogenesis. *J Am Soc Nephrol*. 2016;27:3117–3128. doi: [10.1681/asn.2015050499](https://doi.org/10.1681/asn.2015050499)
44. Khan R, Agrotis A, Bobik A. Understanding the role of transforming growth factor-beta1 in intimal thickening after vascular injury. *Cardiovasc Res*. 2007;74:223–234. doi: [10.1016/j.cardiores.2007.02.012](https://doi.org/10.1016/j.cardiores.2007.02.012)
45. Jiang Z, Tao M, Omalley KA, Wang D, Ozaki CK, Berceli SA. Established neointimal hyperplasia in vein grafts expands via TGF-beta-mediated progressive fibrosis. *Am J Physiol Heart Circ Physiol*. 2009;297:H1200–H1207. doi: [10.1152/ajpheart.00268.2009](https://doi.org/10.1152/ajpheart.00268.2009)
46. Low EL, Baker AH, Bradshaw AC. TGFbeta, smooth muscle cells and coronary artery disease: a review. *Cell Signal*. 2019;53:90–101. doi: [10.1016/j.cellsig.2018.09.004](https://doi.org/10.1016/j.cellsig.2018.09.004)
47. de Vries MR, Parma L, Peters HAB, Schepers A, Hamming JF, Jukema JW, Goumans M, Guo L, Finn AV, Virmani RMJTH, et al. Quax Blockade of vascular endothelial growth factor receptor 2 inhibits intraplaque haemorrhage by normalization of plaque neovessels. *J Intern Med*. 2018;285:59–74. doi: [10.1111/joim.12821](https://doi.org/10.1111/joim.12821)
48. de Jong A, de Jong RCM, Peters EA, Arens R, Jukema JW, de Vries MR, Quax PHA. P300/CBP associated factor (PCAF) deficiency enhances diet-induced atherosclerosis in ApoE3\*Leiden mice via systemic inhibition of regulatory T cells. *Front Cardiovasc Med*. 2021;7:604821. doi: [10.3389/fcvm.2020.604821](https://doi.org/10.3389/fcvm.2020.604821)
49. Grondin CM, Meere C, Castonguay Y, Lepage G, Grondin P. Progressive and late obstruction of an Aorto-coronary venous bypass graft. *Circulation*. 1971;43:698–702. doi: [10.1161/01.cir.43.5.698](https://doi.org/10.1161/01.cir.43.5.698)
50. Chen H, Wang Z, Si K, Wu X, Ni H, Tang Y, Liu W, Wang Z. External stenting for saphenous vein grafts in coronary artery bypass grafting: a meta-analysis. *Eur J Clin Invest*. 2023;53:e14046. doi: [10.1111/eci.14046](https://doi.org/10.1111/eci.14046)
51. Elshafay A, Bendary AH, Vuong HT, Ahmed AR, Mokhtar MA, Soliman AL, Vuong NL, Bestawi IAE, Abdallah NA, Vu VT, et al. Does no-touch technique better than conventional or intermediate saphenous vein harvest techniques for coronary artery bypass graft surgery: a systematic review and meta-analysis. *J Cardiovasc Transl Res*. 2018;11:483–494. doi: [10.1007/s12265-018-9832-y](https://doi.org/10.1007/s12265-018-9832-y)
52. Layton GR, Ladak SS, Abbasciano R, McQueen LW, George SJ, Murphy GJ, Zakkar M. The role of preservation solutions upon saphenous vein endothelial integrity and function: systematic review and UK practice survey. *Cells*. 2023;12:815. doi: [10.3390/cells12050815](https://doi.org/10.3390/cells12050815)
53. Gaudio M, Sandner S, An KR, Dimagli A, Di Franco A, Audisio K, Harik L, Perezgrovas-Olaria R, Soletti G, Fremes SE, et al. Graft failure after coronary artery bypass grafting and its association with patient characteristics and clinical events: a pooled individual patient data analysis of clinical trials with imaging follow-up. *Circulation*. 2023;148:1305–1315. doi: [10.1161/CIRCULATIONAHA.123.064090](https://doi.org/10.1161/CIRCULATIONAHA.123.064090)
54. Wang XW, Zhao XJ, Xiang XY. Gene therapy for vein graft failure. *J Card Surg*. 2013;28:144–147. doi: [10.1111/jocs.12075](https://doi.org/10.1111/jocs.12075)
55. George SJ, Wan S, Hu J, MacDonald R, Johnson JL, Baker AH. Sustained reduction of vein graft neointima formation by ex vivo TIMP-3 gene therapy. *Circulation*. 2011;124:S135–S142. doi: [10.1161/CIRCULATIONAHA.110.012732](https://doi.org/10.1161/CIRCULATIONAHA.110.012732)
56. Wan S, George SJ, Nicklin SA, Yim AP, Baker AH. Overexpression of p53 increases lumen size and blocks neointima formation in porcine interposition vein grafts. *Mol Ther*. 2004;9:689–698. doi: [10.1016/j.ymthe.2004.02.005](https://doi.org/10.1016/j.ymthe.2004.02.005)
57. West NE, Qian H, Guzik TJ, Black E, Cai S, George SE, Channon KM. Nitric oxide synthase (nNOS) gene transfer modifies venous bypass graft remodeling: effects on vascular smooth muscle cell differentiation and superoxide production. *Circulation*. 2001;104:1526–1532. doi: [10.1161/hc3801.095693](https://doi.org/10.1161/hc3801.095693)
58. Mann MJ, Whittemore AD, Donaldson MC, Belkin M, Conte MS, Polak JF, Orav EJ, Ehsan A, Dell'Acqua G, Dzau VJ. Ex-vivo gene therapy of human vascular bypass grafts with E2F decoy: the PREVENT single-centre, randomised, controlled trial. *Lancet*. 1999;354:1493–1498. doi: [10.1016/S0140-6736\(99\)09405-2](https://doi.org/10.1016/S0140-6736(99)09405-2)
59. Lopes RD, Williams JB, Mehta RH, Reyes EM, Hafley GE, Allen KB, Mack MJ, Peterson ED, Harrington RA, Gibson CM, et al. Edifoligide and long-term outcomes after coronary artery bypass grafting: PROject of ex-vivo vein graft ENgineering via transfection IV (PREVENT IV) 5-year results. *Am Heart J*. 2012;164:379–386. doi: [10.1016/j.ahj.2012.05.019](https://doi.org/10.1016/j.ahj.2012.05.019)
60. Alexander JH, Hafley G, Harrington RA, Peterson ED, Ferguson TB Jr, Lorenz TJ, Goyal A, Gibson M, Mack MJ, Gennevois D, et al. Efficacy and safety of edifoligide, an E2F transcription factor decoy, for prevention of vein graft failure following coronary artery bypass graft surgery: PREVENT IV: a randomized controlled trial. *JAMA*. 2005;294:2446–2454. doi: [10.1001/jama.294.19.2446](https://doi.org/10.1001/jama.294.19.2446)
61. McDonald RA, White KM, Wu J, Cooley BC, Robertson KE, Halliday CA, McClure JD, Francis S, Lu R, Kennedy S, et al. miRNA-21 is dysregulated in response to vein grafting in multiple models and genetic ablation in mice attenuates neointima formation. *Eur Heart J*. 2013;34:1636–1643. doi: [10.1093/eurheartj/ehh105](https://doi.org/10.1093/eurheartj/ehh105)
62. Schepers A, Eefting D, Bonta PI, Grimbergen JM, de Vries MR, van Weel V, de Vries CJ, Egashira K, van Bockel JH, Quax PHA. Anti-MCP-1 gene therapy inhibits vascular smooth muscle cells proliferation and attenuates vein graft thickening both in vitro and in vivo. *Arterioscler Thromb Vasc Biol*. 2006;26:2063–2069. doi: [10.1161/01.ATV.0000235694.69719.e2](https://doi.org/10.1161/01.ATV.0000235694.69719.e2)
63. Simons KH, de Vries MR, Peters HAB, Hamming JF, Jukema JW, Quax PHA. The protective role of toll-like receptor 3 and type-I interferons in the pathophysiology of vein graft disease. *J Mol Cell Cardiol*. 2018;121:16–24. doi: [10.1016/j.yjmcc.2018.06.001](https://doi.org/10.1016/j.yjmcc.2018.06.001)
64. Piola M, Prandi F, Bono N, Soncini M, Penza E, Agrifoglio M, Polvani G, Pesce M, Fiore GB. A compact and automated ex vivo vessel culture system for the pulsatile pressure conditioning of human saphenous veins. *J Tissue Eng Regen Med*. 2016;10:E204-215. doi: [10.1002/term.1798](https://doi.org/10.1002/term.1798)
65. Prandi F, Piola M, Soncini M, Colussi C, D'Alessandra Y, Penza E, Agrifoglio M, Vinci MC, Polvani G, Gaetano C, et al. Adventitial vessel growth and progenitor cells activation in an ex vivo culture system mimicking human saphenous vein wall strain after coronary artery bypass grafting. *PLoS One*. 2015;10:e0117409. doi: [10.1371/journal.pone.0117409](https://doi.org/10.1371/journal.pone.0117409)
66. Liu F, Wang X, Hu G, Wang Y, Zhou J. The transcription factor TEAD1 represses smooth muscle-specific gene expression by abolishing myocardin function. *J Biol Chem*. 2014;289:3308–3316. doi: [10.1074/jbc.M113.515817](https://doi.org/10.1074/jbc.M113.515817)
67. Schlegelmilch K, Mohseni M, Kirak O, Pruszk J, Rodriguez JR, Zhou D, Kreger BT, Vasioukhin V, Avruch J, Brummelkamp TR, et al. Yap1 acts downstream of  $\alpha$ -catenin to control epidermal proliferation. *Cell*. 2011;144:782–795. doi: [10.1016/j.cell.2011.02.031](https://doi.org/10.1016/j.cell.2011.02.031)
68. Ebrahimihaei R, McNeill MC, Smith SA, Wray JP, Ford KL, Newby AC, Bond M. Elevated cyclic-AMP represses expression of exchange protein activated by cAMP (EPAC1) by inhibiting YAP-TEAD activity and HDAC-mediated histone deacetylation. *BBA-Mol Cell Res*. 2019;1866:1634–1649. doi: [10.1016/j.bbamcr.2019.06.013](https://doi.org/10.1016/j.bbamcr.2019.06.013)
69. Savorani C, Malinverno M, Seccia R, Maderna C, Giannotta M, Terreran L, Mastrapasqua E, Campaner S, Dejana E, Giampietro C. A dual role of YAP in driving TGF $\beta$ -mediated endothelial-to-mesenchymal transition. *J Cell Sci*. 2021;134. doi: [10.1242/jcs.25137115](https://doi.org/10.1242/jcs.25137115)
70. Liu Y, Li M, Lv X, Bao K, Yu Tian X, He L, Shi L, Zhu Y, Ai D. Yes-associated protein targets the transforming growth factor beta pathway to mediate high-fat/high-sucrose diet-induced arterial stiffness. *Circ Res*. 2022;130:851–867. doi: [10.1161/CIRCRESAHA.121.320464](https://doi.org/10.1161/CIRCRESAHA.121.320464)
71. Pesce M, Duda GN, Forte G, Girao H, Raya A, Roca-Cusachs P, Sluijter JPG, Tschöpe C, Van Linthout S. Cardiac fibroblasts and mechanosensation in heart development, health and disease. *Nat Rev Cardiol*. 2023;20:309–324. doi: [10.1038/s41569-022-00799-2](https://doi.org/10.1038/s41569-022-00799-2)
72. Wang L, Luo JY, Li B, Tian XY, Chen LJ, Huang Y, Liu J, Deng D, Lau CW, Wan S, et al. Integrin-YAP/TAZ-JNK cascade mediates atheroprotective effect of unidirectional shear flow. *Nature*. 2016;540:579–582. doi: [10.1038/nature20602](https://doi.org/10.1038/nature20602)
73. Feng J, Gou J, Jia J, Yi T, Cui T, Li Z. Verteporfin, a suppressor of YAP-TEAD complex, presents promising antitumor properties on ovarian cancer. *Onco Targets Ther*. 2016;9:5371–5381. doi: [10.2147/ott.s109979](https://doi.org/10.2147/ott.s109979)
74. Mia MM, Cibi DM, Abdul Ghani SAB, Song W, Tee N, Ghosh S, Mao J, Olson EN, Singh MK. YAP/TAZ deficiency reprograms macrophage phenotype and improves infarct healing and cardiac function after myocardial infarction. *PLoS Biol*. 2020;18:e3000941. doi: [10.1371/journal.pbio.3000941](https://doi.org/10.1371/journal.pbio.3000941)

75. de Jong A, Sier VQ, Peters HAB, Schilder NKM, Jukema JW, Goumans M, Quax PHA, de Vries MR. Interfering in the ALK1 pathway results in macrophage-driven outward remodeling of murine vein grafts. *Front Cardiovasc Med*. 2021;8:784980. doi: [10.3389/fcvm.2021.784980](https://doi.org/10.3389/fcvm.2021.784980)
76. Baganha F, de Jong RCM, Peters EA, Voorham W, Jukema JW, Delibegovic M, de Vries MR, Quax PHA. Atorvastatin pleiotropically decreases intraplaque angiogenesis and intraplaque haemorrhage by inhibiting ANGPT2 release and VE-cadherin internalization. *Angiogenesis*. 2021;24:567–581. doi: [10.1007/s10456-021-09767-9](https://doi.org/10.1007/s10456-021-09767-9)
77. Parma L, Peters HAB, Sluiter TJ, Simons KH, Lazzari P, de Vries MR, Quax PHA. bFGF blockade reduces intraplaque angiogenesis and macrophage infiltration in atherosclerotic vein graft lesions in ApoE3\*Leiden mice. *Sci Rep*. 2020;10:15968. doi: [10.1038/s41598-020-72992-7](https://doi.org/10.1038/s41598-020-72992-7)
78. Jackson ML, Bond AR, George SJ. Mechanobiology of the endothelium in vascular health and disease: in vitro shear stress models. *Cardiovasc Drugs Ther*. 2023;37:997–1010. doi: [10.1007/s10557-022-07385-1](https://doi.org/10.1007/s10557-022-07385-1)
79. Jeremy JY, Gadsdon P, Shukla N, Vijayan V, Wyatt M, Newby AC, Angelini GD. On the biology of saphenous vein grafts fitted with external synthetic sheaths and stents. *Biomaterials*. 2007;28:895–908. doi: [10.1016/j.biomaterials.2006.10.023](https://doi.org/10.1016/j.biomaterials.2006.10.023)
80. Mehta D, George SJ, Jeremy JY, Izzat MB, Southgate KM, Bryan AJ, Newby AC, Angelini GD. External stenting reduces long-term medial and neointimal thickening and platelet derived growth factor expression in a pig model of arteriovenous bypass grafting. *Nat Med*. 1998;4:235–239. doi: [10.1038/nm0298-235](https://doi.org/10.1038/nm0298-235)
81. Yang Q, Lei D, Huang S, Yang Y, Jiang C, Shi H, Chen W, Zhao Q, You Z, Ye X. A novel biodegradable external stent regulates vein graft remodeling via the hippo-YAP and mTOR signaling pathways. *Biomaterials*. 2020;258:120254. doi: [10.1016/j.biomaterials.2020.120254](https://doi.org/10.1016/j.biomaterials.2020.120254)
82. Yla-Herttuala S, Baker AH. Cardiovascular gene therapy: past, present, and future. *Mol Ther*. 2017;25:1095–1106. doi: [10.1016/j.ymthe.2017.03.027](https://doi.org/10.1016/j.ymthe.2017.03.027)
83. Zhou Z, Chen W, Cao Y, Abdi R, Tao W. Nanomedicine-based strategies for the treatment of vein graft disease. *Nat Rev Cardiol*. 2024. doi: [10.1038/s41569-024-01094-y](https://doi.org/10.1038/s41569-024-01094-y)
84. Wang Y, Wang L, Wise JTF, Shi X, Chen Z. Verteporfin inhibits lipopolysaccharide-induced inflammation by multiple functions in RAW 264.7 cells. *Toxicol Appl Pharmacol*. 2020;387:114852. doi: [10.1016/j.taap.2019.114852](https://doi.org/10.1016/j.taap.2019.114852)
85. Wei C, Li X. Verteporfin inhibits cell proliferation and induces apoptosis in different subtypes of breast cancer cell lines without light activation. *BMC Cancer*. 2020;20:1042. doi: [10.1186/s12885-020-07555-0](https://doi.org/10.1186/s12885-020-07555-0)
86. Kuramoto K, Yamamoto M, Suzuki S, Sanomachi T, Togashi K, Seino S, Kitanaka C, Okada M. Verteporfin inhibits oxidative phosphorylation and induces cell death specifically in glioma stem cells. *FEBS J*. 2020;287:2023–2036. doi: [10.1111/febs.15187](https://doi.org/10.1111/febs.15187)
87. Dobin A, Davis CA, Schlesinger F, Drenkow J, Zaleski C, Jha S, Batut P, Chaisson M, Gingeras TR. STAR: ultrafast universal RNA-seq aligner. *Bioinformatics (Oxford, England)*. 2013;29:15–21. doi: [10.1093/bioinformatics/bts635](https://doi.org/10.1093/bioinformatics/bts635)
88. Langmead B, Salzberg SL. Fast gapped-read alignment with bowtie 2. *Nat Methods*. 2012;9:357–359. doi: [10.1038/nmeth.1923](https://doi.org/10.1038/nmeth.1923)
89. Liao Y, Smyth GK, Shi W. featureCounts: an efficient general purpose program for assigning sequence reads to genomic features. *Bioinformatics (Oxford, England)*. 2014;30:923–930. doi: [10.1093/bioinformatics/btt656](https://doi.org/10.1093/bioinformatics/btt656)
90. Chiesa M, Colombo GI, Piacentini L. DaMiRseq-an R/Bioconductor package for data mining of RNA-Seq data: normalization, feature selection and classification. *Bioinformatics (Oxford, England)*. 2018;34:1416–1418. doi: [10.1093/bioinformatics/btx795](https://doi.org/10.1093/bioinformatics/btx795)
91. Smyth GK, Michaud J, Scott HS. Use of within-array replicate spots for assessing differential expression in microarray experiments. *Bioinformatics (Oxford, England)*. 2005;21:2067–2075. doi: [10.1093/bioinformatics/bti270](https://doi.org/10.1093/bioinformatics/bti270)
92. Ashburner M, Ball CA, Blake JA, Botstein D, Butler H, Cherry JM, Davis AP, Dolinski K, Dwight SS, Eppig JT, et al. Gene ontology: tool for the unification of biology. The Gene Ontology Consortium. *Nat Genet*. 2000;25:25–29. doi: [10.1038/75556](https://doi.org/10.1038/75556)
93. Zhou Y, Zhou B, Pache L, Chang M, Khodabakhshi AH, Tanaseichuk O, Benner C, Chanda SK. Metascape provides a biologist-oriented resource for the analysis of systems-level datasets. *Nat Commun*. 2019;10:1523. doi: [10.1038/s41467-019-09234-6](https://doi.org/10.1038/s41467-019-09234-6)
94. Shannon P, Markiel A, Ozier O, Baliga NS, Wang JT, Ramage D, Amin N, Schwikowski B, Ideker T. Cytoscape: a software environment for integrated models of biomolecular interaction networks. *Genome Res*. 2003;13:2498–2504. doi: [10.1101/gr.1239303](https://doi.org/10.1101/gr.1239303)
95. Piola M, Prandi F, Fiore GB, Agrifoglio M, Polvani G, Pesce M, Soncini M. Human saphenous vein response to trans-wall oxygen gradients in a novel ex vivo conditioning platform. *Ann Biomed Eng*. 2016;44:1449–1461. doi: [10.1007/s10439-015-1434-0](https://doi.org/10.1007/s10439-015-1434-0)
96. Krom YD, Pires NM, Jukema JW, de Vries MR, Frants RR, Havekes LM, van Dijk KW, Quax PH. Inhibition of neointima formation by local delivery of estrogen receptor alpha and beta specific agonists. *Cardiovasc Res*. 2007;73:217–226. doi: [10.1016/j.cardiores.2006.10.024](https://doi.org/10.1016/j.cardiores.2006.10.024)